Palaeogeography, Palaeoclimatology, Palaeoecology 675 (2025) 113088

Contents lists available at ScienceDirect

Palaeogeography, Palaeoclimatology, Palaeoecology

journal homepage: www.elsevier.com/locate/palaeo

# Diverse dinosaur tracks from the Upper Jurassic – Lower Cretaceous Chacarilla Formation of Quebrada de Arcas, northeast Chile: Evidence of high ichnodiversity in an arid palaeoenviroment

Vincenzo Gesualdi [a,*], Matteo Belvedere [a], Marko Yurac [b], Dorothee Hippler [c], Nejla Hurem [c], Christian Salazar [d], Javiera Mendez [d], Christian A. Meyer [e,f]

[a] Dipartimento di Scienze della Terra, Università degli Studi di Firenze, via G. la Pira 4, 50121 Firenze, Italy
[b] Unidad de Patrimonio Paleontológico, Consejo de Monumentos Nacionales, Av. Huérfanos 1515, 7500000 Providencia, Santiago de Chile, Chile
[c] Graz University of Technology, Institute of Applied Geosciences, Rechbauerstraße 12/EG, 8010 Graz, Austria
[d] Facultad de Ciencias, Escuela de Geología, Universidad Mayor, A. Manuel Montt 367, 7500000 Providencia, Santiago de Chile, Chile
[e] Department of Environmental Sciences, University of Basel, Bernoullistr. 32, 4056 Basel, Switzerland
[f] Museo de Historia Natural Alcide d'Orbigny, Avenida Potosi N-1458, Cochabamba, Bolivia

ARTICLE INFO

Editor: H Falcon-Lang

*Keywords:*
Dinosaur tracks
*Abelichnus astigerrae*
Chacarilla Formation
Gondwana
Jurassic-Cretaceous boundary

ABSTRACT

We report diverse dinosaur tracks from siltstone to fine-grained sandstone facies of the Chacarilla Formation, Quebrada de Arcas of northeast Chile. Track-bearing surfaces were studied using 3D modelling and false-colour depth maps, derived from UAV photographs. Five morphotypes are identified based on morphology and morphometric criteria. Morphotype I comprises rounded tracks with a consistent narrow-gauge and resembles the sauropod ichnogenus, *Parabrontopodus*; diplodocids or titanosaurids are probable trackmakers. Morphotype II is assigned to the theropod ichnotaxon *Abelichnus astigerrae* and comprises some of the largest theropod tracks ever recorded from South America with a maximum footprint length of 51 cm; the trackmaker was most likely a large carcharodontosaurid, such as *Giganotosaurus carolinii*. Morphotype III is an indeterminate theropod track, which shows a distinctive and prominent metatarsal impression, but does not closely match any ichnotaxon although it bears some morphometrical affinity to *Changpeipus carbonicus*. The Morphotypes IV and V both belong to small-sized theropod trackmakers, and resemble Grallatoridae and *Kayentapus*-like forms, respectively. Additional theropod material cannot be assigned to specific morphotypes or trackmakers, due to poor preservation. Our findings show the existence of three distinct size classes (small, medium and large) of theropod morphotypes and point to a high ichnodiversity at the Jurassic-Cretaceous transition in the subtropical arid environments of Gondwana.

## 1. Introduction

This study aims to describe and classify new dinosaur tracks from the Chacarilla Fm. of the Quebrada de Arcas, Chile (Fig. 1). The presence of dinosaur footprints in the Chacarilla Fm. from this locality has previously been documented by Galli and Dingham (1962). We present new tracks and trackways discovered during our field work in 2023. This study updates the dinosaur track record with 9 new track-bearing surfaces and describes a total of 94 new tracks from this locality. This documents the high potential for further discoveries in already-known sites, due to the use of advanced methodologies in vertebrate ichnology. The exact age of the Chacarilla Fm. is unknown. The formation has a diachronous upper limit and is Late Jurassic to Early Cretaceous in age. Stratigraphic correlations (Charrier et al., 2007) suggest a Kimmeridgian to Early Cretaceous minimum age for the upper Chacarilla Fm. According to Blanco et al. (2000), the presence of tracks of ornithopod dinosaurs in the upper part of the Chacarilla Fm. at Quebrada Chacarilla indicates an Early Cretaceous age for these levels. However, the absence of any picture or drawing of these ornithopod tracks in Blanco et al. (2000) leaves this hypothesis untestable. Since the first report, several

* Corresponding author.
*E-mail addresses:* vincenzo.gesualdi@unifi.it (V. Gesualdi), matteo.belvedere@unifi.it (M. Belvedere), myurac@monumentos.gob.cl (M. Yurac), dorothee.hippler@tugraz.at (D. Hippler), nejla.hurem@student.tugraz.at (N. Hurem), christian.salazar@umayor.cl (C. Salazar), javiera.mendez@mayor.cl (J. Mendez), chris.meyer@unibas.ch (C.A. Meyer).

https://doi.org/10.1016/j.palaeo.2025.113088
Received 20 January 2025; Received in revised form 6 June 2025; Accepted 6 June 2025
Available online 9 June 2025
0031-0182/© 2025 The Authors. Published by Elsevier B.V. This is an open access article under the CC BY license (http://creativecommons.org/licenses/by/4.0/).

studies have been made at different localities in the Chacarilla Fm. and the underlying Majala Fm. (Rubilar-Rogers, 2008 and references therein); the latest discoveries are known from Quebrada Huatacondo (Yurac et al., 2022).

## 2. Geographical and geological setting

### 2.1. Geographical context of the Quebrada de Arcas

The present study was carried out in the Quebrada de Arcas, located in the Antofagasta region in Chile (Fig. 1). The closest settlement is Quillagua, at the border of the Antofagasta and Tarapacá regions along the Panamericana Highway 5. Supplementary Table 1 includes the

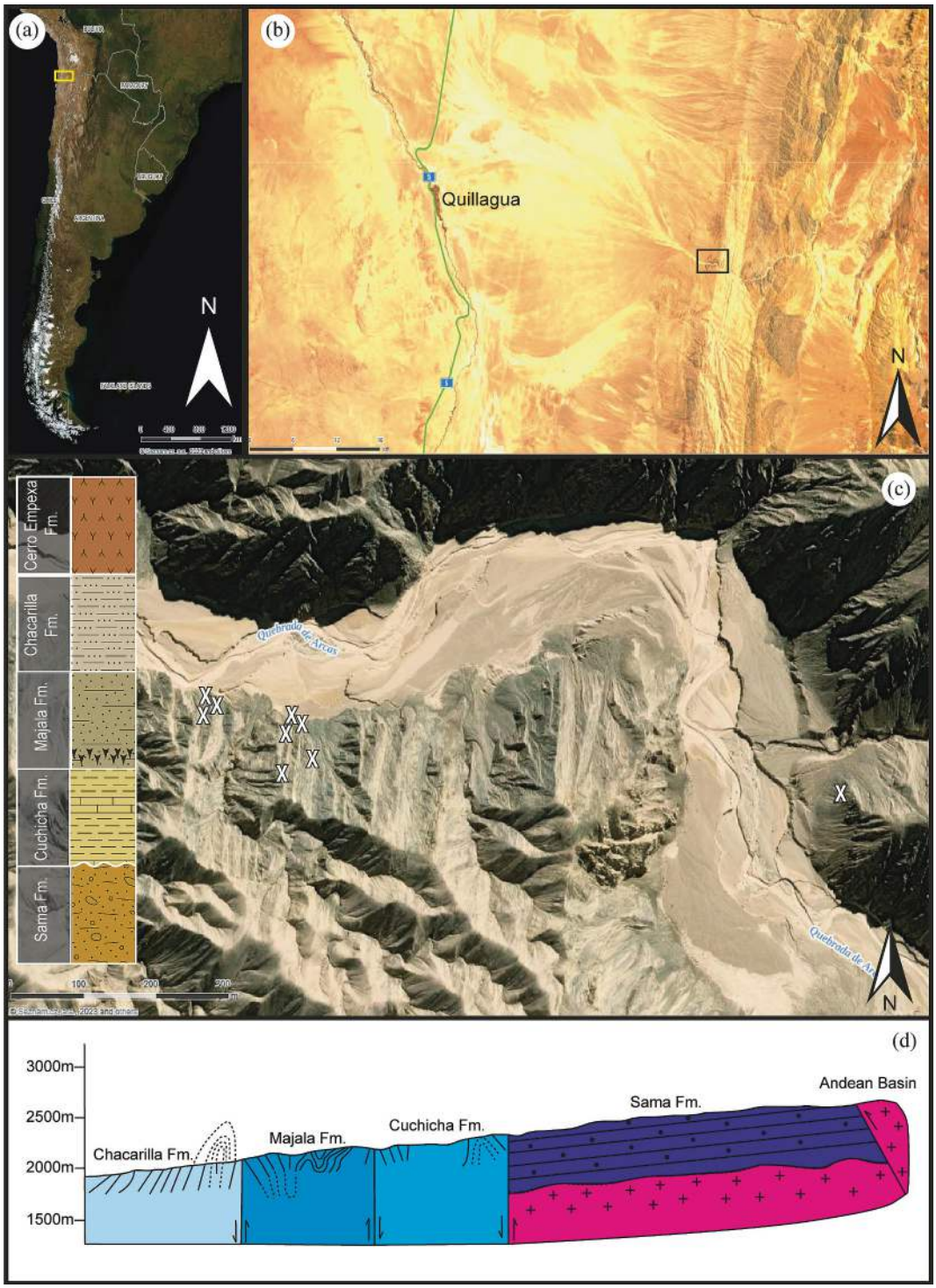


**Fig. 1.** Location of the Quebrada de Arcas tracksite. (a) Overview of Chile; (b) close-up on the Quillaga village with the Quebrada de Arcas tracksite in the black square; (c) study area in the Quebrada de Arcas with the schematic log of the formations. X represents the track-bearing surfaces (QA/1, QA/9, QA/12, QA/14, QA/15, QA/17, QA/20, QA/21, QA/22); (d) schematic cross-section of the Quebrada de Arcas. Redrawn from Sepulveda et al. (2023).

precise coordinates of the track-bearing layers in the Quebrada de Arcas working area (21°S-22°S and 69°W).

### 2.2. Geological setting of the Quebrada de Arcas

The general geological setting at ~20–22° S has been described by Habel et al. (2023). The basement of the Andean Basin is formed by Precambrian and Paleozoic magmatic and metamorphic rocks. The Mesozoic (Triassic-Cretaceous) is represented by sedimentary deposits, followed by a Middle to Late Cenozoic (Oligocene-Quaternary) sedimentary and volcanic cover. The Quebrada de Arcas area was part of a back-arc basin that formed during the beginning of the Andean Cycle between the Late Jurassic-Early Cretaceous (Charrier et al., 2007). A cross-section of the Quebrada de Arcas is given in Fig. 1d. Dinosaur tracks were exclusively found in the Chacarilla Fm., which is in the midsection of the Mesozoic sedimentary succession that crops out in the area.

The lowermost and first unit of the succession along the Quebrada de Arcas is the Sama Fm. (Upper Triassic, Orrego, 1992) made up of sandstones and conglomerates of an alluvial-fluvial to lacustrine environment, postulated to be formed under semi-arid conditions (Orrego, 1992). The second unit would constitute the marine transgressive Pucana Fm. (Hettangian-Sinemurian, Aguilef et al., 2019), which is however not exposed in the Quebrada de Arcas. In fact, there is an

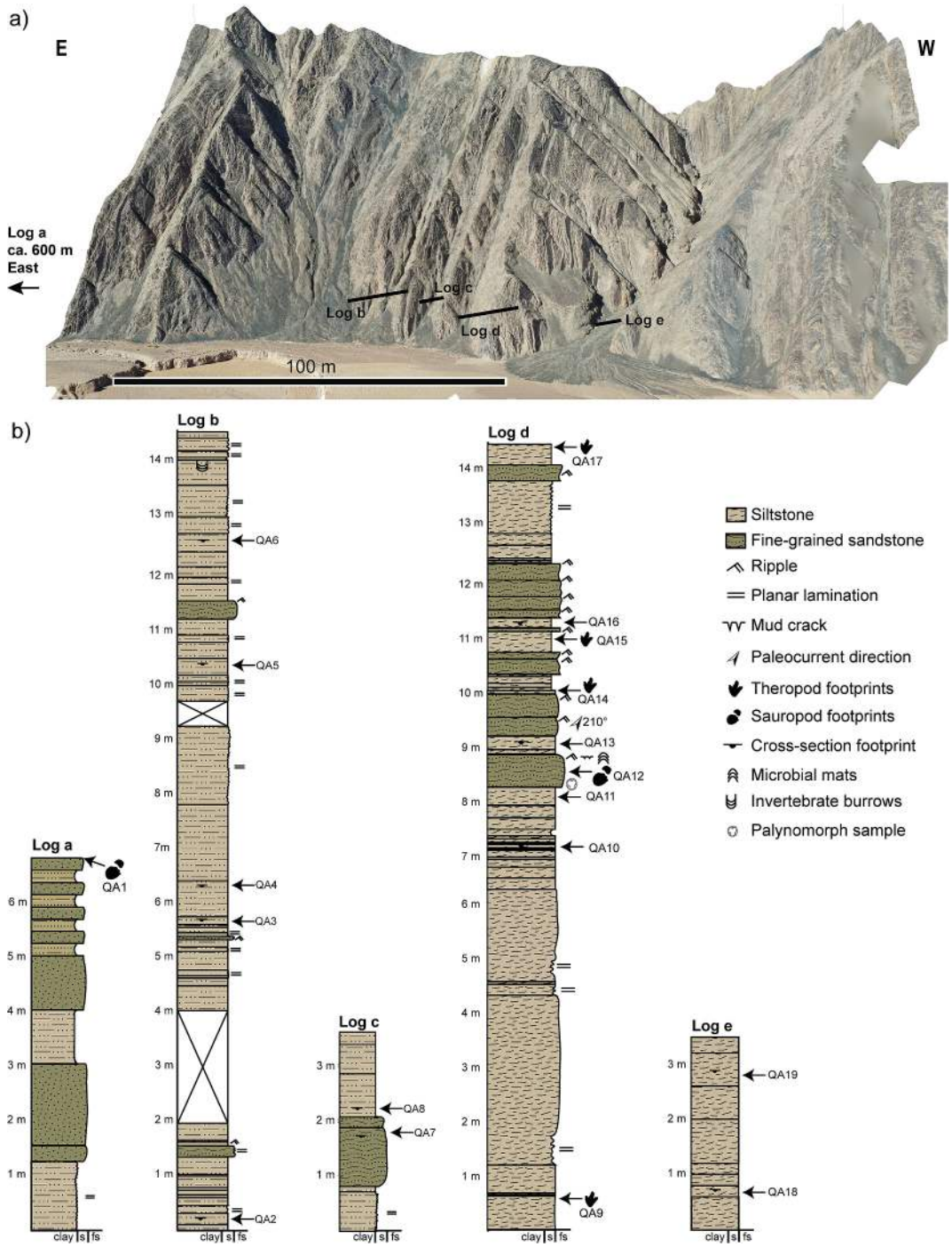


**Fig. 2.** Stratigraphical setting of the Quebrada de Arcas tracksite. Logs (a, b, c, d, e) show in detail the position of the 22 track-bearing surfaces.

angular unconformity between the Sama Fm. and the overlying Cuchicha Fm. (Pliensbachian-Oxfordian, Aguilef et al., 2019). The latter consists of shallow-water, high-energy limestones (e.g. packstones, floatstones and rudstone) from a carbonate platform (Aguilef et al., 2019). In terms of stratigraphic continuity, it follows the Majala Fm. (Upper Oxfordian, Garcia, 1967) which is made up of marine to deltaic silt- and fine sandstones with intercalated gypsum levels. Both the sedimentological structures and the fossil record (e.g. marine fossils at the base and dinosaur tracks at the top of the formation, Galli and Dingham, 1962), indicate a shallowing upward sequence (Blanco and Tomlison, 2013). The overlying Chacarilla Fm. (Upper Oxfordian-Lower Cretaceous, Galli and Dingham, 1962) was proposed to represent the beginning of a continental terrigenous sedimentation. This unit is composed of dark grey to brownish siltstones and fine sandstones originally interpreted as deposits of a meandering fluvial system (Galli and Dingham, 1962) and now considered to be deposited in a distal alluvial plain (Mendez, 2024). We collected samples for detrital zircon dating which are being processed. The updated geochronological and sedimentological data will be part of an upcoming paper. The Chacarilla Fm. terminates with an angular unconformity with volcanic magmatic arc deposits of the Cerro Empexa Fm (Upper Cretaceous, Tomlinson et al., 2001). U—Pb dating from volcanic zircons indicate an age between 83 Ma and 68 Ma (Blanco and Tomlison, 2013) for the Cerro Empexa Fm., corresponding to the Campanian to Maastrichtian stages.

### 2.3. *The Chacarilla Fm. in the Quebrada de Arcas*

The studied succession of the Chacarilla Fm. in the Quebrada de

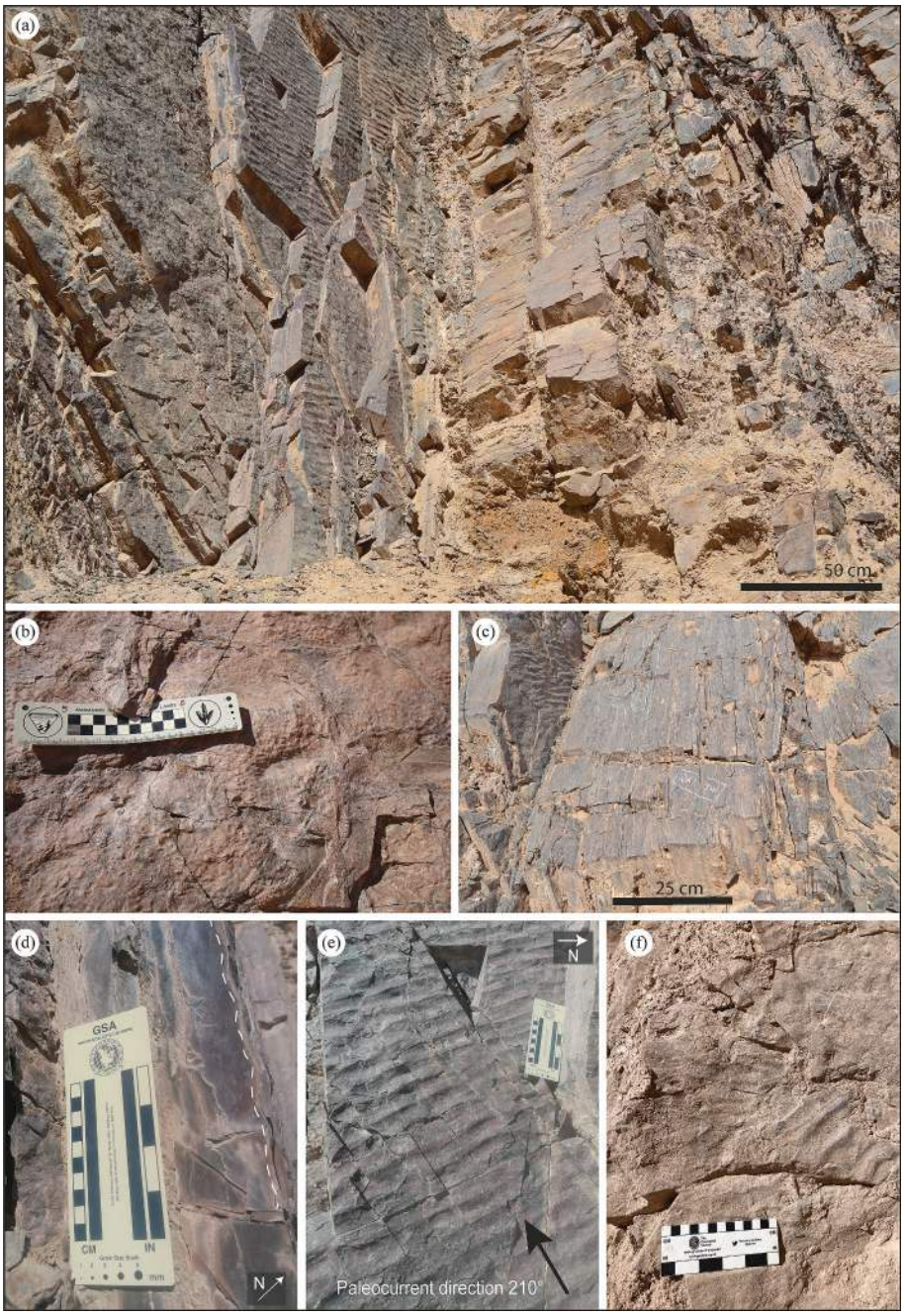


**Fig. 3.** Sedimentary structures in the Chacarilla Fm. Ripple marks (a, d, e), planar lamination (a, c), microbial mats from surface QA12 (b), *Ophiomorpha* (f) and cross-section dinosaur tracks (c). Scale bars are: 50 cm in (a), 18 cm in (b), 25 cm in (c), 10 cm in (d, e, f).

Arcas is about 300 m thick and is composed of a monotonous succession of dark greyish to brownish siltstones and fine-grained sandstones (Fig. 2). Mineralogically, they are composed of quartz (50–55 wt.-%), alkali feldspar (ca. 25 wt.-%) and illite, mica and chlorite (20–25 wt.-%) with minor amounts of hematite. They can be classified as arkosic to litharenitic sandstones (Pettijohn et al., 1972) or wacke to litharenitic sandstones (Herron, 1988). They have an ICV (index of compositional variability, Cox et al., 1995) of less than 1, which means that they are compositionally mature and are deposited in a tectonically quiescent, cratonic environment, where sediment recycling is active.

Bed thickness of the Chacarilla Fm. silt- and sandstones varies along the succession, with mainly thin-bedded layers to a few intercalated medium-bedded layers. The strata dip direction ranges between 290°-300° N with a dip angle between 70°-75°. Asymmetric and symmetric ripples are the most frequent sedimentological structures on the exposed surfaces of the fine-grained sandstones of the Chacarilla Fm., whereas mud-cracks, invertebrate burrows and microbial mats predominantly occur on the surfaces of the silty levels (Fig. 3).

### 2.4. Stratigraphical description

Five logs were measured around the track surfaces and levels with tracks preserved in cross-section (Fig. 2). Fig. 2A shows the relative position of 4 of the measured logs (b-e), whereas the 'a' log position corresponds to that of surface QA1 (Fig. 1); the track-bearing surfaces QA/20, QA/21 and QA/22 were elevated and inaccessible, whilst their lower part, which could have been suitable for logging, was covered by recent alluvial deposits. They are visible in the field and from the 3D model (Supplementary Table 1), however the texture resolution of the outcrop's cross-section is not high enough for a detailed stratigraphical log, considering that the layers are cm-thick.

#### 2.4.1. Log a

The succession consists of 6.7 m of alternating silt and very fine sandstones. The strata occur in meter-thick levels, exhibiting minimal or no evidence of lamination. The uppermost layer of the succession is constituted by the first track-bearing paleosurface (QA/1). (This log is not on the 3D in Fig. 2, since its position is farther east than the model. The position of this log is instead visible in Fig. 1c).

#### 2.4.2. Log b

The succession consists of 14.5 m of siltstones. It was not possible to measure certain parts of the section, due to the presence of approximately 2.5 m of slope debris which covered the strata. The thickness of the individual layers varies significantly, ranging from centimetre-thick to metre-thick. The sedimentary structures that are visible include planar lamination and asymmetric ripples, with the former being more abundant than the latter. Lamination is more pronounced in the upper part of the section, while the rest display it, but less frequently. The invertebrate burrows are located at a point close to the uppermost part of the section, at approximately 13.9 to 14 m. Five distinct levels of cross-section footprints are identified in this area (QA/2, QA/3, QA/4, QA/5 and QA/6).

#### 2.4.3. Log c

The succession consists of 3.6 m of siltstone. Lamination is only observable in the middle of the first layer. Symmetric ripples are found in just one layer and have a direction of 230°. Two footprint layers (QA/7 and QA/8) are observed in the proximity of this stratum.

#### 2.4.4. Log d

The succession consists of 14.1 m of laminated and massive siltstones. Strata vary from cm to m-thick. The two main sedimentological structures are planar lamination and ripples. The asymmetric ripples exhibit an overall direction of 210°. However, certain layers exhibit ripples with two distinct directions. It should be noted that directional measurements were not feasible for these layers, due to their inaccessibility. The layer containing the sauropod tracks exhibits the presence of bubbly microbial mat structures (Fig. 3b). While such an association is not uncommon, it is the most evident indication of microbial mats within the study area. A total of nine footprints levels (QA/9, QA/10, QA/11, QA/12, QA/13, Q/14, QA/15, QA/16 and QA/17) were identified, including some vertebrate non-dinosaurian tracks yet to be formally described (QA/11). A single sample was selected for palynomorph analysis (QA/P/1).

#### 2.4.5. Log e

The succession consists of 3.5 m of siltstones. Lamination is the only observable feature (including the layer that exhibits footprints). Two footprints on the same level are present (QA/18 and QA/19).

### 2.5. Potential paleoenvironment of the Chacarilla Fm

Galli and Dingham (1962) originally interpreted the Chacarilla Fm. as deposits of meandering rivers. Recent studies, focussed on the Quebrada Huatacondo (Mendez, 2024), revised the potential paleoenvironment of the Majala Fm. and the Chacarilla Fm. According to sedimentological and petrological observations and analysis, track-bearing levels in both formations match with the facies of a distal alluvial floodplain (Mendez, 2024). The very fine to fine-grained nature of the sedimentary rocks, their high compositional maturity and the existence of sedimentary structures of low-energy environments corroborates this lithofacies interpretation. The lithology, sedimentary structures and abundance of dinosaur track horizons in the Quebrada de Arcas confirm Mendez (2024) re-interpretation of the depositional setting of the Chacarilla Fm. Petrological and geochemical analysis (Hurem et al., 2023) seem to further confirm this interpretation.

Cheirolepidiacean-dominated assemblage in the Chacarilla Fm are reported by Moreno et al. (2024), which were interpreted as indicating temporally arid conditions. The only sample analysed for palynomorphs in our study however did not reveal any pollen, palynomorph or organic matter. This can either be interpreted as evidence of aridity of the depositional environment, or it might also be due to diagenesis and the alteration and decomposition of organic matter. The results of a single sample are not sufficient to make any further interpretations.

Using the ichnological record of Cretaceous sauropod tracks in South America (Tomaselli et al., 2021) there is a clear link between tracksites and floodplains as the main paleoenvironmental setting. Other occurrences are possible also in other continental environments (fluvial and lacustrine systems) as well as in coastal environments (marginal-marine).

## 3. Materials and methods

### 3.1. Materials

The studied material was labelled using an acronym combining the locality (QA = Quebrada de Acras) and progressive numbering from 1, which was the lowermost track-bearing surface, to 22, the uppermost of the track-bearing surfaces (e.g., QA/17 indicated the 17th track bearing surfaces found moving towards the top of the succession). The designation for the tracks distinguished between isolated tracks (IT) and trackways (Tw). Both isolated tracks and trackways were numbered progressively along the surface and with their stratigraphical position. 'L' and 'R' identify left and right tracks, respectively. 'P' and 'M' were used for pes and manus, respectively. Therefore, e.g., QA/17 Tw7-RP2 indicates the second right pes impression of trackway 7, found on surface 17 in the Quebrada de Arcas tracksite.

All tracks and trackways were studied and analysed from digital models derived from pictures made by drone (UAV photos), because the inclination of the surfaces and the friability of the rocks made direct access too hazardous. Measurements of dip direction and dip angle of

the track-bearing surfaces were made where surfaces were accessible.

All tracks are described following Leonardi (1987) and Lallensack et al. (2025). Track and trackways parameters have been measured as in Fig. 4. The anterior triangle (AT) has been measured to indicate the protrusion of digit III. This parameter is often referred as "mesaxony" (after Lockley, 2009) and currently is still used ambiguously (see: Romano et al., 2018; Lallensack et al., 2025). The gauge was estimated using the trackway ratio of Romano et al. (2007). Trackmaker speed has been estimated using Alexander's (1976) formula ($v = 0.25\ g^{0.5} * SL^{1.67} * h^{1.17}$), where the hip height has been calculated as h = 4.586PL (Gonzalez-Riga, 2011) for sauropod, h = 4,9PL for large theropods and h = 4,5PL for small theropods (Thulborn, 1990). Gait has been measured as SL/h wherever possible. Track fidelity (sensu Lallensack et al., 2025), or morphological preservation (sensu Marchetti et al., 2019) was assigned using the scale of Marchetti et al. (2019), based on the previous scale by Belvedere and Farlow (2016). This scale is based on the visible morphological characteristics of the tracks, assigning a numerical value from 0 to 3, where 0 is barely recognisable as a track, and 3 corresponds to "elite tracks" (sensu Lockley, 1994). Their interpretation is reported in the track descriptions (from Sections 4.1.1 to 4.1.9). All measurements are available in Supplementary Table 2.

One sample (QA/P/1) was taken for palynomorph analysis (from surface QA/11). The palynofacies analysis was done with 201 g of sediment by the palynological lab at the University of Florence. The procedure used follows Riding (2021).

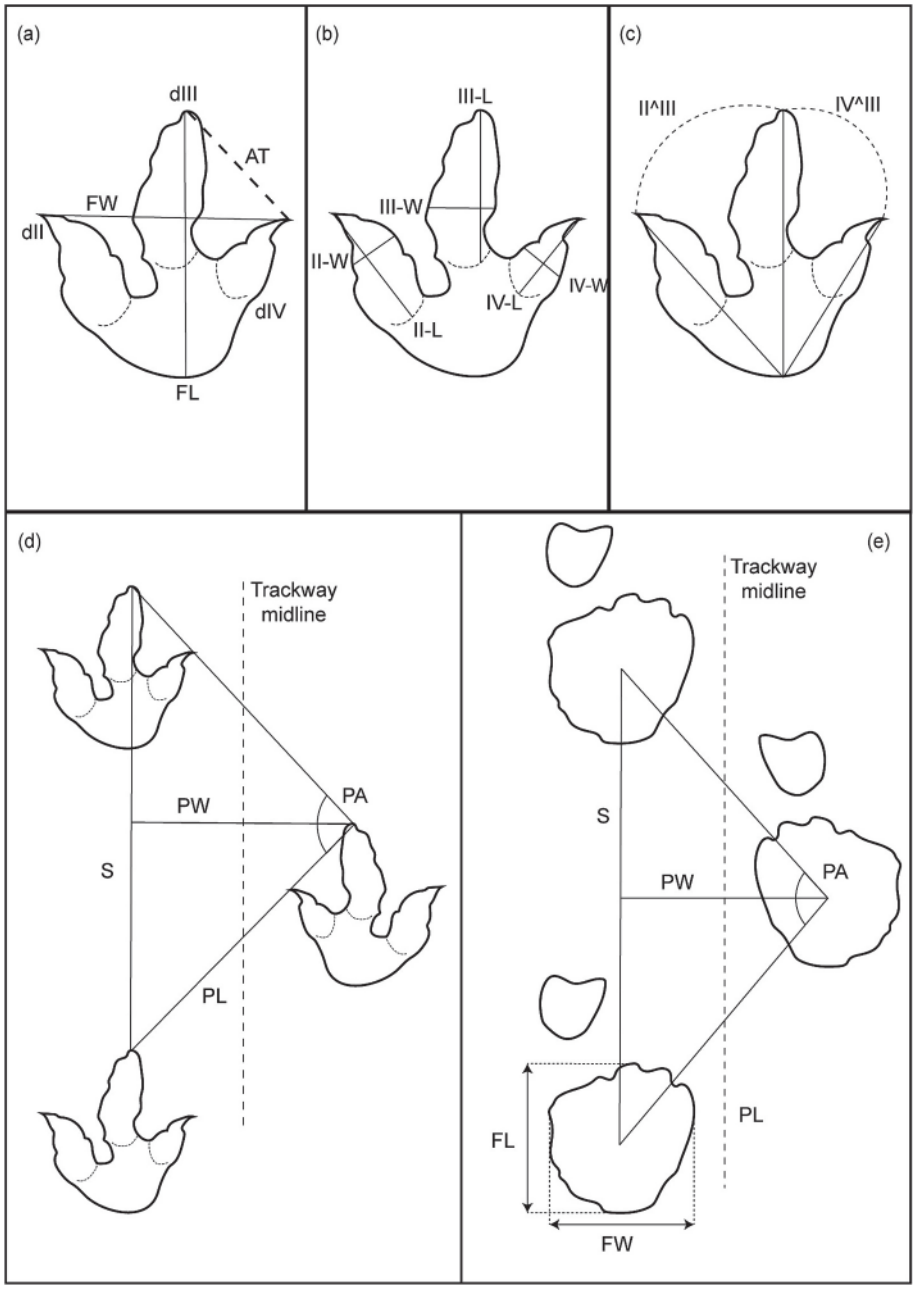


**Fig. 4.** Tracks and trackway parameter measurements. (a) Measurements referred to tridactyl footprint length (FL), width (FW) and anterior triangle (AT); (b) measurements referred to tridactyl digit length (II-L, III-L and IV-L), digit width (II-W. III-W and IV-W); (c) measurements for interdigital angles (II^III and IV^IV); (d) trackway measurements for tridactyl tracks: pace length (PL), pace width (PW), pace angulation (PA) and stride (S); (e) trackway measurements for quadruped tracks: pace length (PL), pace width (PW), pace angulation (PA) and stride (S).

### 3.2. 3D data acquisition and elaboration

Three different drones were used to take UAV photos: a DJI Mavic 2 Pro (20 Mpixel), a DJI Mavic Air 2 (48-Mpixel) and a DJI Mini 2 (12-Mpixel). In addition, when possible, photographs were also taken with DSLR cameras: a Nikon D3100 (14.2 Mpixel) equipped with an 18-55 mm lens, and a Canon EOS 70D (20.1 Mpixel) equipped with a 18–135 mm STL lens.

The 3D photogrammetric models were generated using Agisoft Metashape (v. 1.8.6), while the depth maps and contour-line maps were made with CloudCompare (v. 2.12.4) following Lallensack et al. (2021). Outline drawings and measurements were made from the 3D models in CorelDraw (v. 24.5). All 3D models and associated metadata used in this work can be downloaded from the link provided in Supplementary Table 1, following Falkingham et al. (2018).

## 4. Results

### 4.1. Description of tracks and outcrops

Our study identified 94 tracks distributed along 10 track-bearing surfaces. In addition, 12 track-bearing surfaces could be detected in cross-section. 24 tracks have been attributed to theropods (11 isolated track and 13 on trackways) and 70 to sauropods (28 isolated and 42 arranged in trackways). From the 'true' track-bearing surfaces (see Supplementary Table 1 for the type of track-bearing level), only one (QA/21) preserves both sauropod and theropod tracks. The other surfaces preserve either theropod (QA/9, QA/14, QA/15, QA/17) or sauropod tracks (QA/1, QA/12, QA20, QA/22). The following sections describe each of the track-bearing layers in stratigraphic order, from the lower to the upper part of the section.

#### 4.1.1. QA/1

QA/1 is an outcrop including two separate trampled surfaces (Figs. 5 and 6) of the same level. A total of 27 quadrupedal tracks are preserved, arranged in four trackways (Tw1-Tw4) and two isolated tracks (IT1, IT2). None of the tracks display distinctive features except for Tw1-LP4, Tw4-LP1, Tw4-LP2 and Tw4-RP2, where digits are visible. Fidelity is 0.5 for all the tracks except for Tw4-RP2 and Tw4-LP2, where fidelity is 1.

**Trackway Tw1**: This trackway is composed of 5 manus and pes print tracks, with only 2 clear pes-manus couples (Fig. 5). The total trackway length is 3.7 m. The mean PL is 97 cm. Mean PW is 80 cm. Pes tracks are slightly positively rotated (+7°), with respect to the trackway midline. Due to the poor fidelity of the tracks, the gauge, gait and velocity are a rough estimate only. The gauge is very narrow (PRT = 53.96 %); the gait is <2 (1.13), indicating walking behaviour according to Thulborn (1990). The average speed is 3.33 km/h. The trackway direction is towards 66° (NE).

**Trackway Tw2**: This trackway consists of 5 tracks (1 pes-manus couple) located in the centre of the surface (Fig. 5). The trackway direction intersects with Tw3, but since there is no overlap or visible interaction it is impossible to reconstruct the order of superimposing. The total trackway length is about 3.5 m. The mean PL is 121.05 cm. Mean PW is 80 cm but with only one value. Pes tracks are rotated outward (+13°), with respect to the trackway midline, while the only manus tracks (Tw2-RM1) have a strong inward rotation (−25°). The gauge is narrow (PRT = 54 %) and similar to Tw1. Mean gait is lower than 2 (0.64), indicating a walking behaviour. The average speed is 1.83 km/h. Trackway direction is 0° (N).

**Trackway Tw3**: This trackway consists of 6 tracks (1 pes-manus couple) located in the upper part of the surface (Fig. 5). As mentioned above, the direction of Tw2 shows that it would intersect with Tw3, but the order of superposition cannot be determined. The total trackway length is about 7.2 m. The mean PL is 112.5 cm. Mean PW is 52 cm with only one value. The mean rotation is outward and slightly pronounced (+11°). The gauge (PRT = 57.44 %) slightly differs compared to the other trackways of the same surface. Only one gait measurement was possible, indicating walking behaviour, due to its value being lower than 2 (0.99). The average speed is 3.82 km/h. Trackway direction is 90° (E).

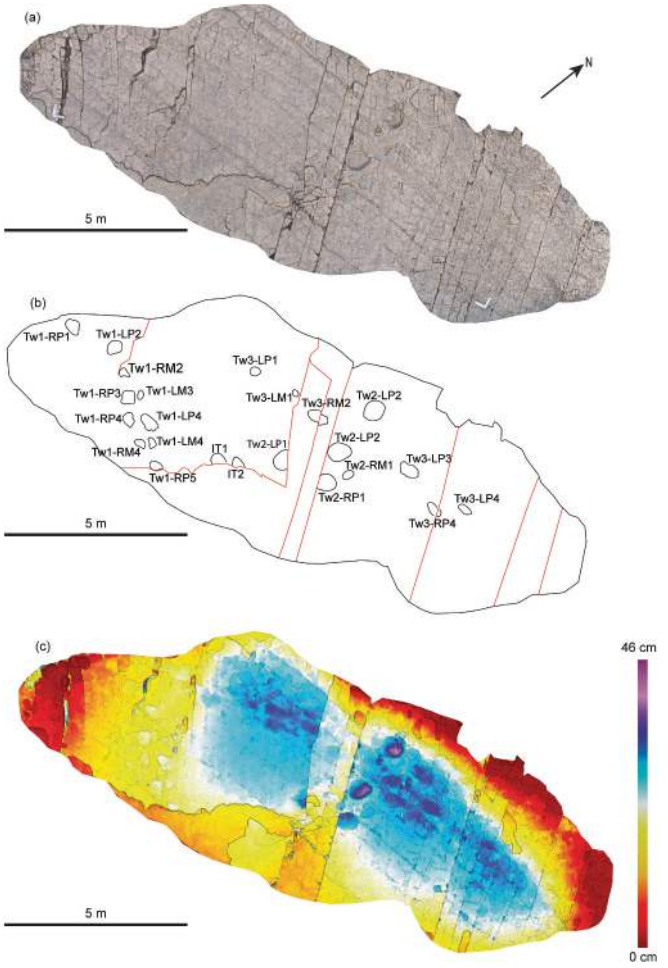


**Fig. 5.** Overview of the first part of QA1. (a) Surface photo; (b) outline drawing; (c) depth map. Scale bar is 5 m.

**Trackway Tw4**: This trackway consists of 4 pes tracks located in the right part of the second separate part of the surface composing QA/1 (Fig. 6). The total trackway length cannot be estimated, since the first and last track of the trackway are incomplete and in a faulted area. Both mean PL and mean PW cannot be estimated. The mean rotation is outward and slightly pronounced (+8°). The gauge (PRT = 53.45 %) is like Tw1 and Tw2. No gait measurements were possible. In this case, speed cannot be estimated due to the absence of S values. Trackway direction is 127° (SE).

#### 4.1.2. QA/9

QA/9 has seven tridactyl tracks both isolated (IT3, IT4, IT5) and composing trackway Tw5 (Fig. 7). Metatarsal impressions are visible in two tracks (Tw5-LP2 and Tw5-RP2). IT3 has digits that are similar in width and have small angles between the digits. IT4 has more divergent digits and the pad impressions are clearly visible showing a 2–3-2 formula with the foot pad being visible. Those two digits and IT5 are not deeply impressed when compared to Tw5 tracks. Tw5-LP2 and Tw5-RP2 are the other remarkable tracks on this surface. The pad formula is probably 2–2-2. The main feature of this track is the preserved metatarsal impression. In addition, Tw5-LP2 may have digit I slightly impressed. Fidelity is 1 except for tracks IT4 and Tw5-LP2, where it is 2.

**Trackway Tw5** is a continuous trackway made up of 4 tridactyl tracks, two of which are only partially preserved (Fig. 7). Trackway

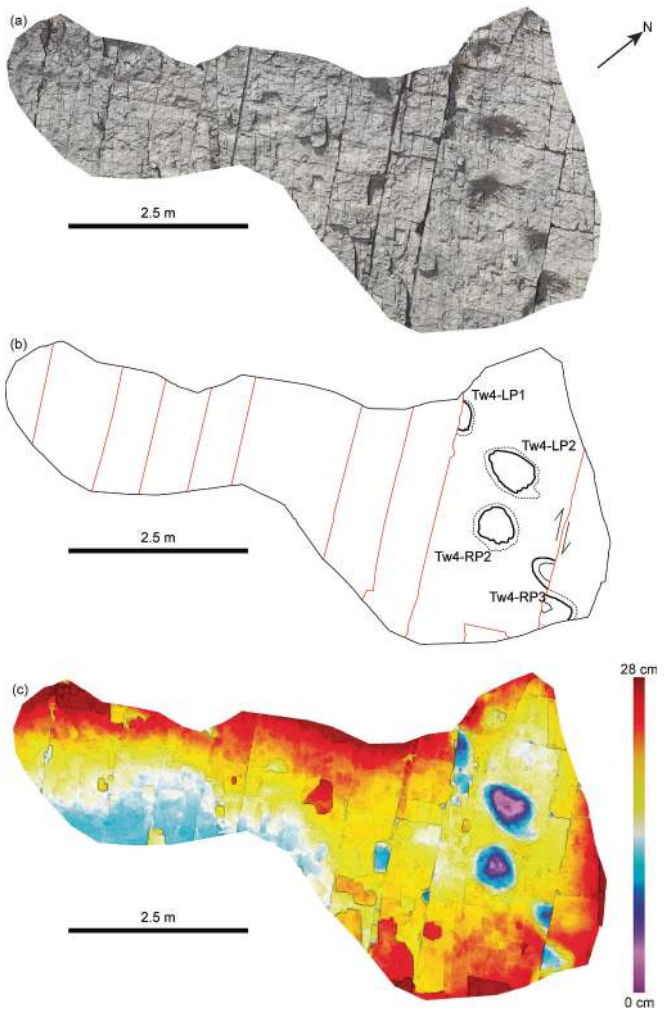


**Fig. 6.** Overview of the second part of QA1. (a) Surface photo; (b) outline drawing; (c) depth map. Scale bar is 2.5 m.

length is 3 m. Mean PL is 36.05 cm, given solely by the value of one track. Mean PW is 24.6. Tracks are slightly outward rotated with respect to the midline (+4°). The AT l/w ratio is expressed by values of 0.35 and 0.44. No gait measurements were possible. Speed cannot be estimated. Trackway direction is 150° (SE). Fidelity is 1.

#### 4.1.3. QA/12

QA/12 has only one isolated large track (IT6) with a well-developed mud rim (Fig. 8). The surface also shows evidence of microbial mats in the lowest part of the surface (Fig. 3b). Just below this surface is a level (QA11) that contains a trackway of an as yet undetermined very small tetrapod. The fidelity is 1.5.

#### 4.1.4. QA/14

QA/14 is a shallow isolated large tridactyl track, consisting only of digits II and III and the claw mark of digit IV (Fig. 9). The only parameter measured was FW, with a value of approximately 37.5 cm, indicating a medium-sized trackmaker. No other consideration can be assessed on this track, due to the suboptimal preservation. Fidelity is 1.

#### 4.1.5. QA/15

QA/15 displays five isolated tridactyl tracks (IT8-IT12) on a highly fractured surface (Fig. 10). Track IT8 has the outline preserved but neither pad impressions nor other anatomical features are visible. Isolated track IT9 is a left pes track with well-preserved digit IV where the two pads are visible in depth maps. The outline is preserved for most of the track except for digit III, where only one pad and a presumed claw mark are visible. Digit II seems not to be preserved at all, except for one clear pad impression where the base of the digit should be. The last but most remarkable track is IT10, which belongs to a large-sized trackmaker with digits longer than wider, the edges of the digits pointing to the exterior in II and IV while to the interior for digit III, having a pad formula of 2–3-2 and claw impressions for all digits. Track quality is 1 (sensu Marchetti et al., 2019) for all tracks on this surface except for IT10. This track, even if incomplete, has well-preserved anatomical impression and its fidelity is 2.

#### 4.1.6. QA/17

QA/17 shows two parallel trackways (Tw6, Tw7), both made by large tridactyl trackmakers (Fig. 11). Trackway Tw7 overlaps Tw6. The means of FL and FW are 48.3 cm and 41.1 cm. Except for track Tw6-RP2, all the others show pad impressions and claw marks. Those tracks have a pad formula of 2–3-2 for the digits and one single pad impression in the foot. Claws marks are visible in all the digits. Digits are longer than wider, AT l/W ranges from 0.27 to 0.46. Pace length is similar in both trackways, with a mean of 152.1 cm for Tw6 and 152.8 cm for Tw7. There is also similarity in pace angulation, which is 158° for Tw6 and 152° for Tw7. Tracks of this surface are the best preserved of the study. They are clear and sharp, with all the anatomical impressions of pads and claws, along with complete digits, being clearly visible. Track fidelity ranges from 2 to 2.5 (except for Tw6-LP2, which is incomplete with a fidelity of 0.5).

**Trackway Tw6** is made of 3 tridactyl tracks and the trackway is overlapped by Tw7 (Fig. 11). Trackway length is roughly 3.5 m. Mean PL is 48.3 cm. Mean PW is 43.5 based on one track measured. The mean rotation is low but slightly different between the two measured values (+12° and + 3°). The AT l/w ratio is low (0.27). No gait measurements were possible. Speed cannot be estimated. Trackway direction is 82° (NE).

**Trackway Tw7** is made of 3 tridactyl tracks that overlap a track of Tw6 (Fig. 11). Trackway length is roughly 3.4 m. Mean PL is 48.43 cm. Mean PW is 45.7 cm. The mean rotation is low, more pronounced in Tw7-RP1 (+20°) than Tw7-LP2 (+10°) and Tw7-RP3 (+3°). Also, for tracks AT l/w ratio remains very low, ranging from 0.311 to 0.43. The mean gait is 1.28 (walking). The average speed is 6.53 km/h. Trackway direction is 82° (NE).

#### 4.1.7. QA/20

QA/20 has 10 quadrupedal tracks, all attributable to a large-sized trackmaker (Fig. 12). On this surface only IT16, Tw8-RP1 and Tw8-LP2 have digits preserved and these are the better-preserved tracks here. Fidelity is 0.5.

**Trackway Tw8** consists of 4 pes tracks located in the middle part of the surface (Fig. 12). The total trackway length is about 2.4 m. Means PL and PW could not be measured. The mean rotation is outward and quite pronounced (+35°). The gauge (PRT =89.95 %) is the widest recorded in this study. Mean gait is 0.35, indicating walking behaviour due to its value being lower than 2. The average speed is 0.83 km/h. Trackway direction is 233° (SW).

#### 4.1.8. QA/21

QA/21 is made up by two non-continuous surfaces (Figs. 13 and 14) where 35 tracks from both sauropods and theropods can be seen. This is the only case of a surface displaying the two different groups of dinosaurs together. Quadrupedal sauropod tracks rarely bear any remarkable features except for IT31 and Tw10-LP3, where both digits and the expulsion rim are visible. Tridactyl theropod tracks are not usually well-preserved, lacking digits or some other part of the track. In IT34 pads in digit III and the foot can be seen and digit IV points to the exterior. Fidelity is 0.5.

**Trackway Tw9** consists of 6 pes tracks located in the upper left part of the surface (Fig. 13). The total trackway length is 3.8 m. Mean PL is

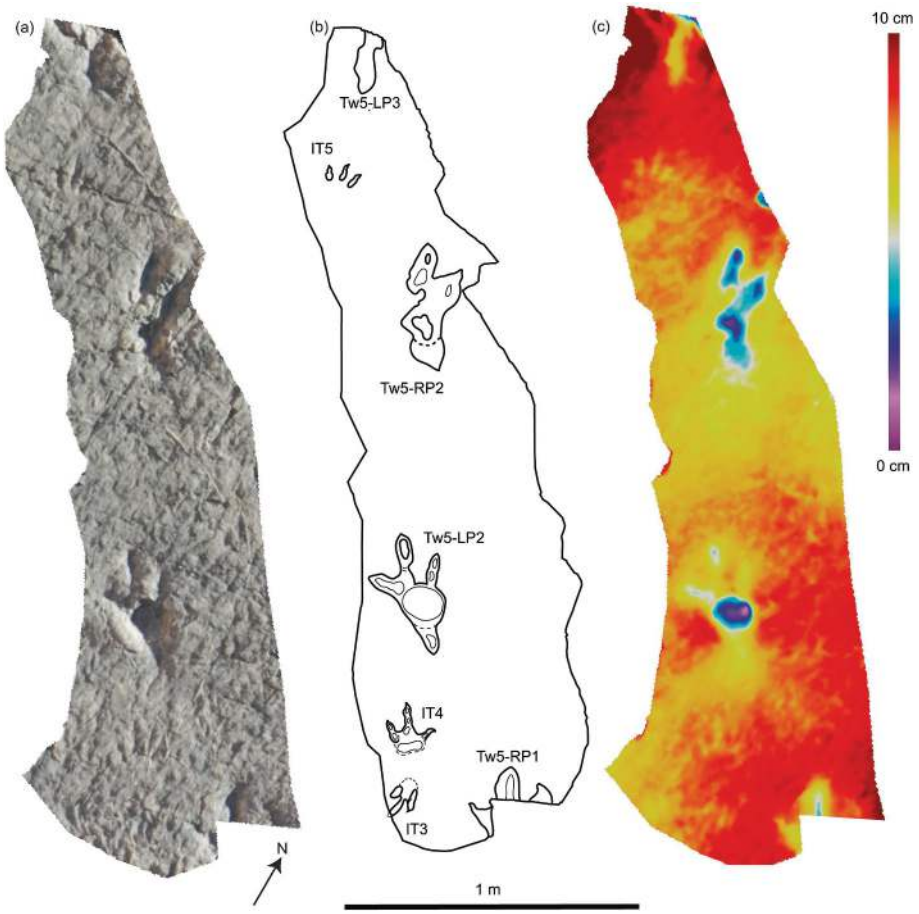


**Fig. 7.** Overview of QA9. (a) Surface photo; (b) outline drawing; (c) depth map. Scale bar is 1 m.

85.22 cm and mean PW is 39.1 cm. The mean rotation is outward and slightly pronounced (+6°). The gauge (PRT = 45.21 %) is indicative of a narrow gauge of trackway. The mean gait is 0.7 (< 2 means walking). The average speed is 2.08 km/h. Trackway direction is 142° (SE).

**Trackway Tw10** is made by 7 tracks (1 pes-manus couple) located close to Tw9 in the upper part of the surface (Fig. 13). The total trackway length is 4.4 m. Mean PL is 124.7 cm, and mean PW is 54.5 cm. The mean rotation is outward (+9°). The gauge (PRT = 34.68 %) is the lowest measured among all tracks. The mean gait is <2 (0.58) and this indicates that the trackmaker was walking. Speed is estimated at 1.39 km/h. Trackway direction is 163° (SE).

**Trackway Tw11** is made by 3 tridactyl tracks (Fig. 14). Trackway length is 2.1 m. Mean PL is 37.6 cm, given by the value of just one track. Mean PW is 33.3 cm. The mean rotation is low, if not absent (<2°). AT l/w ratio expresses values of 0.37 and 0.54. This is the only tridactyl trackway with a gait measurement (0.94) that shows a walking behaviour. The average speed is 3.46 km/h. Trackway direction is 119° (SE).

#### 4.1.9. QA/22

QA/22 has just two tracks, specifically one pes and one manus (Fig. 15). The preservation is poor, mainly as a result of the high level of fracturing of the surface, which affects the track depth when seen in 3D maps. No anatomical evidence or other features are visible. Both tracks from the surface have a low fidelity of 0.5.

### 4.2. Track analysis

Based on morphological parameters, five morphotypes are defined in this study (Fig. 16); attributions of each track and trackways are provided in Supplementary Table 2.

***Morphotype I*** is characterized by rounded tracks longer than wide (FW/FL ranges from 0.45 to 0.98), except for four tracks where the value is higher than 1, ranging from 1 to 1.17. There are too few tracks with digits to be considered a consistent feature. Tw4 shows a wide gauge (89.95 %), while all the others are very narrow gauge (ranging 34.6 to 54.0) with minimal rotation (except for tracks in Tw8) and stride ranging from 109.1 to 187 cm across all the various trackways included in this morphotype.

The tracks attributed to this morphotype are all the rounded tracks, both as isolated tracks and from the quadrupedal trackways (Tw1, Tw2, Tw3, Tw4, Tw8, Tw9, Tw10). This morphotype has been attributed to a sauropod trackmaker.

***Morphotype II*** is made up of tridactyl tracks equal in length and width (FW/FL ranging from 0.908 to 1.006) and low AT l/w ratio (ranging from 0.27 to 0.43). Differences in digits shows that digit III is the largest, followed, in order, by digits II and IV. There is no difference in depth between digits of the same track. Some digits tend to be deeper than others, simply because the tracks overlap during the impression phase, making these digit impressions unreliable. Interdigital angles are asymmetrical with IIˆIII (29°-44°) and IVˆIII (62°-71°). Trackways show a narrow gauge with pace angulation (PA) values indicating straight walking with stride (S) ranging from 145.1 to 159.1 cm with minor rotation (R) of maximally 20°. This morphotype has been attributed to a theropod trackmaker.

***Morphotype III*** consists of tridactyl tracks characterized by the presence of both a metatarsal impression and a potential digit I impression (clearly visible in Tw5-LP2 from Fig. 7). Due to this partial preservation the measurement of FW/FL has been done for just one track (Tw5-LP2), giving a value of 0.7. Even if other tracks cannot be measured, they are longer than wide. AT l/W is low, with values of 0.35

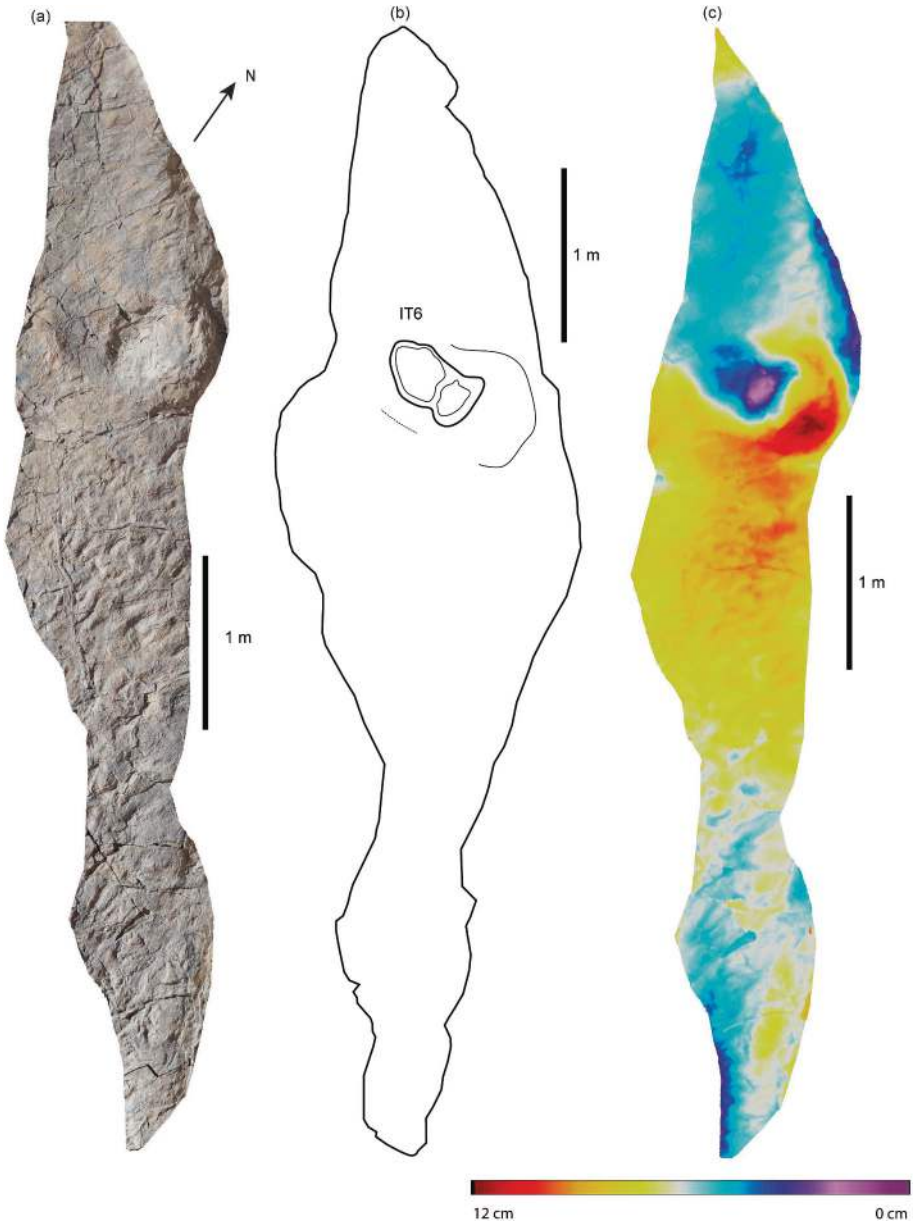


**Fig. 8.** Overview of QA12. (a) Surface photo; (b) outline drawing; (c) depth map. Scale bar is 1 m.

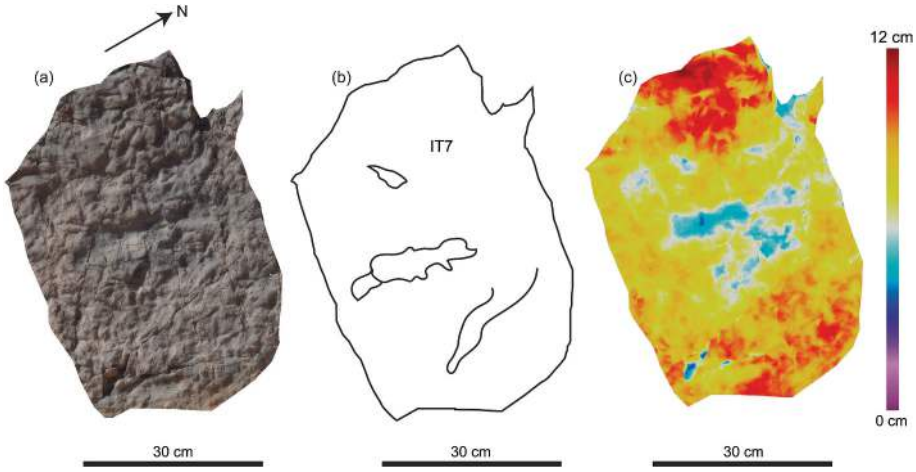


**Fig. 9.** Overview of QA14. (a) Surface photo; (b) outline drawing; (c) depth map. Scale bar is 30 cm.

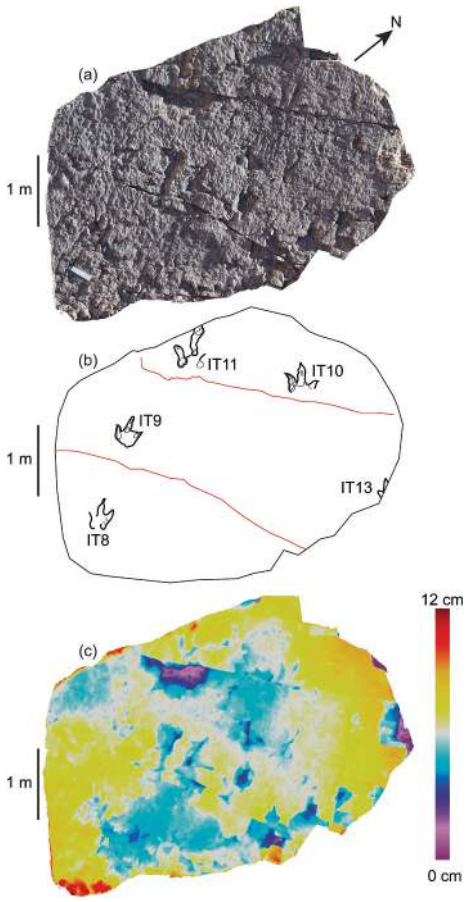


**Fig. 10.** Overview of QA15. (a) Surface photo; (b) outline drawing; (c) depth map. Scale bar is 1 m.

and 0.44 on just two tracks where it was possible to measure. Digit III is the longest with II and IV being of similar length but different width (IV-W > II-W). Inconsistency in track preservation and the resulting lack of complete tracks also meant that it was not possible to measure all tracks and track parameters. Pace length (PL) has been measured once with value of 102.6 cm. Rotation (R) is low with just two values of 3° and 6°. The tracks attributed to this morphotype are: Tw5-RP1, Tw5-LP2, Tw5-RP2, Tw5-LP3. This morphotype has been attributed to a theropod trackmaker.

***Morphotype IV*** include only the tridactyl track IT3 (surface QA9). The tracks are almost double in length the width (value of FW/FL of 0.503). It must be considered that the outline of the track is not completely preserved, so this measurement is plausible but not certain. AT l/W is 0.75. No major anatomical structure is visible. Digital length order is digit III, digit II and digit IV. Width of the digits is roughly the same for all three. The digit divergence is low in both digit II and digit IV. To this morphotype belongs the track IT3. This morphotype has been attributed to a theropod trackmaker.

***Morphotype V*** contains only the tridactyl track IT4 (surface QA9). This track is slightly longer than it is wide (FW/FL 0.91) with an AT l/W of 0.479. The values of the single digits show almost a similar width, with significative differences only in length. The digit divergence is more pronounced for digit IV than digit II. Pads are well preserved in digit II and digit III. To this morphotype belongs the track IT4. This morphotype has been attributed to a theropod trackmaker.

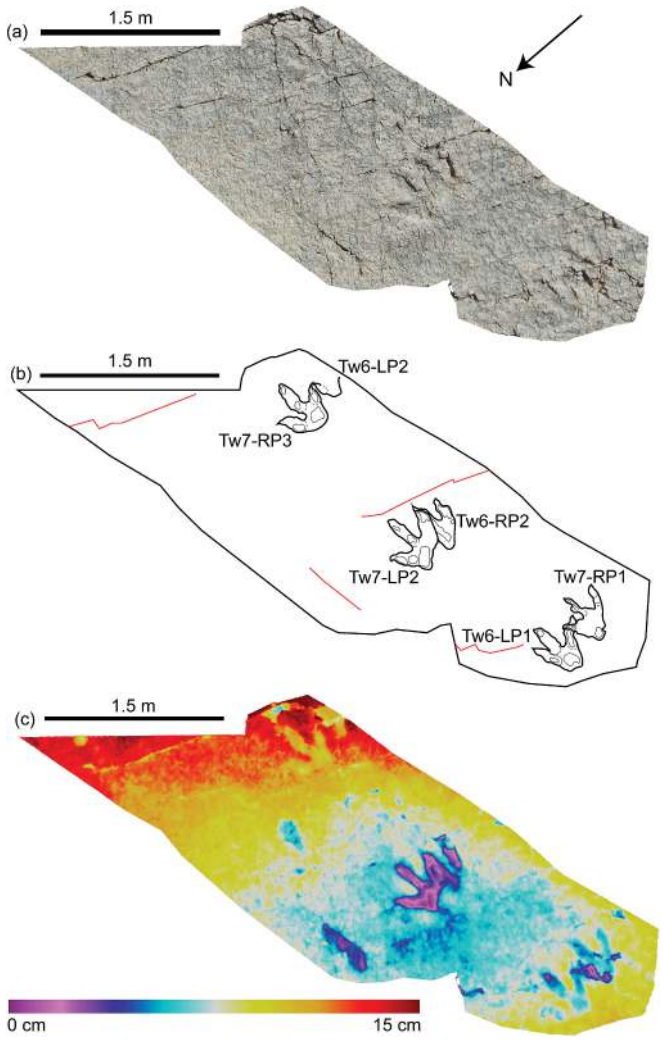


**Fig. 11.** Overview of QA17. (a) Surface orthophoto derived from 3D model; (b) outline drawing; (c) false-colour depth map. Scale bar is 1.5 m.

## 5. Discussion

### 5.1. Morphotype interpretation

Dinosaur tracksites in the Upper Jurassic to Lower Cretaceous from South America are widely known (e.g. Apesteguía and Gallina, 2011; de Valais et al., 2012; Leonardi, 1994; Leonardi and De Souza Carvalho, 2021; Mesa and Perea, 2015; Moreno-Sánchez et al., 2011).

In Chile, the fossil record of non-avian dinosaurs from the Late Jurassic-Early Cretaceous is less abundant, particularly when compared to the ichnological one (Yurac et al., 2025). The first Chilean dinosaur tracks were described by Galli and Dingham (1962) and Casamiquela and Fasola (1968). More recent studies began two decades ago (Moreno and Pino, 2002; Moreno et al., 2004; Rubilar-Rogers, 2008; Rubilar-Rogers et al., 2012) and are ongoing (Moreno et al., 2024; Yurac et al., 2022; Yurac et al., 2025). These papers form the basis with which to understand the context of the Quebrada de Arcas footprints within a Gondwanan framework. As Rubilar-Rogers et al. (2012) highlighted, the ichnosites in Chile offer a valuable glimpse into the diverse range of this group, both in terms of variety and size. The tracks described herein reinforce this record. Five distinct morphotypes have been recorded at this one site, pointing to a great ichnodiversity. The findings of this study demonstrate the trackmakers' range in both type (sauropod and theropod) and size (small to medium to large-sized for the theropods), thereby confirming the thesis of Rubilar-Rogers et al. (2012) and

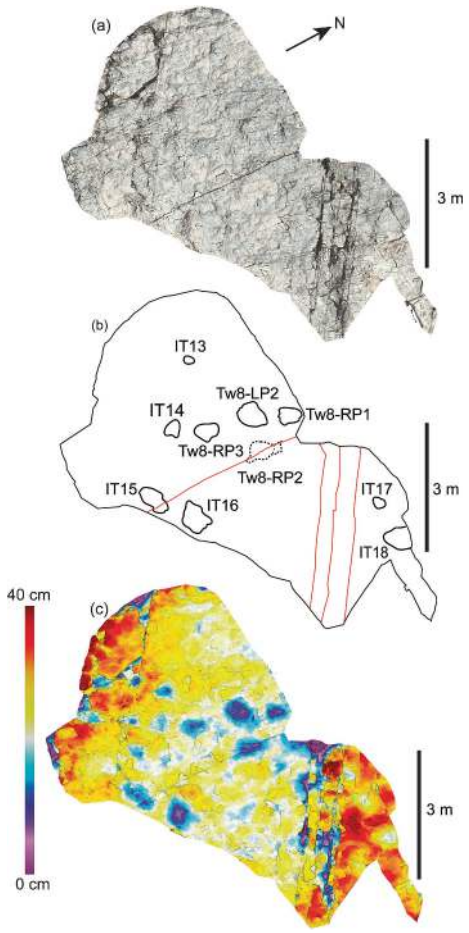


**Fig. 12.** Overview of QA20. (a) Surface photo; (b) outline drawing; (c) false-colour depth map. Scale bar is 3 m.

concomitantly improving our knowledge of the dinosaurs that were present at this time period in Gondwana.

Rubilar-Rogers (2008) identified two different morphotypes for the tracks in the Quebrada Chacarilla. Morphotype A has a long digit III with digit II and IV being about half of digit III. Morphotype B has digit II and IV about 1/3 of digit III.

The identification of five different morphotypes within this study was made with consideration for the differences in track morphology, size, interdigital angles and trackmaker (for Morphotype I). Projecting the tracks for the FL/FW ratio vs. the AT l/w ratio and the FL/FW ratio vs. divarication angles (IIIˆII, IIIˆIV, IIˆIV) reinforces the idea of four distinct tridactyl morphotypes (Fig. 17). Similarities of those morphometric parameters for Morphotype II and Morphotype V do not pose a problem, since there is high disparity in track size (avg. FL is 48.38 cm for Morphotype I and is 18.2 cm for Morphotype V) and morphology (e.g. heel pad is rounded in Morphotype II while it is wider than longer in Morphotype V), rendering a clear distinction between the two morphotypes (Fig. 17).

### 5.1.1. Morphotype I

No significant detail is preserved in the sauropod tracks of Morphotype I, and no definitive ichnotaxonomical assignment can be made. The lack of consistent well-defined pes and manus tracks make the narrow gauge of the trackways the only available parameter for an ichnotaxonomic classification. The ichnotaxonomic classification has been made with consideration for seven Late Jurassic-Early Cretaceous ichnotaxa (Fig. 18b-d). The following taxa were excluded for a variety of reasons: *Sauropodichnus* (Calvo, 1991) was excluded for the wide gauge and very poor morphology. *Calorckosauripus* (Meyer et al., 2018) was excluded for its difference in morphology and heteropody. *Breviparopus* (Dutuit and Ouazzou, 1980) shows a big difference in morphology and heteropody, despite its comparable gauge. *Galinhapodus* (Santos et al., 2024) was excluded for the lack of an evident claw mark on digit one of its manus track and the very wide gauge. *Titanopodus* (González-Riga and Calvo, 2009) was excluded for difference in morphology and the narrow gauge. Previous studies (Moreno and Pino, 2002; Moreno et al., 2004), classified sauropod tracks from the Chacarilla Fm. and the Majala Fm. as *Brontopodus* (Farlow et al., 1989) and *Parabrontopodus* (Lockley et al., 1994). However, these footprints still cannot be confidently interpreted at the genus level because of the poor preservation. The classification of tracks from Morphotype I is *Parabrontopodus*-like.

### 5.1.2. Morphotype II

The ichnotaxonomical assignation of Morphotype II has been done considering the large-sized theropods from South America, since the

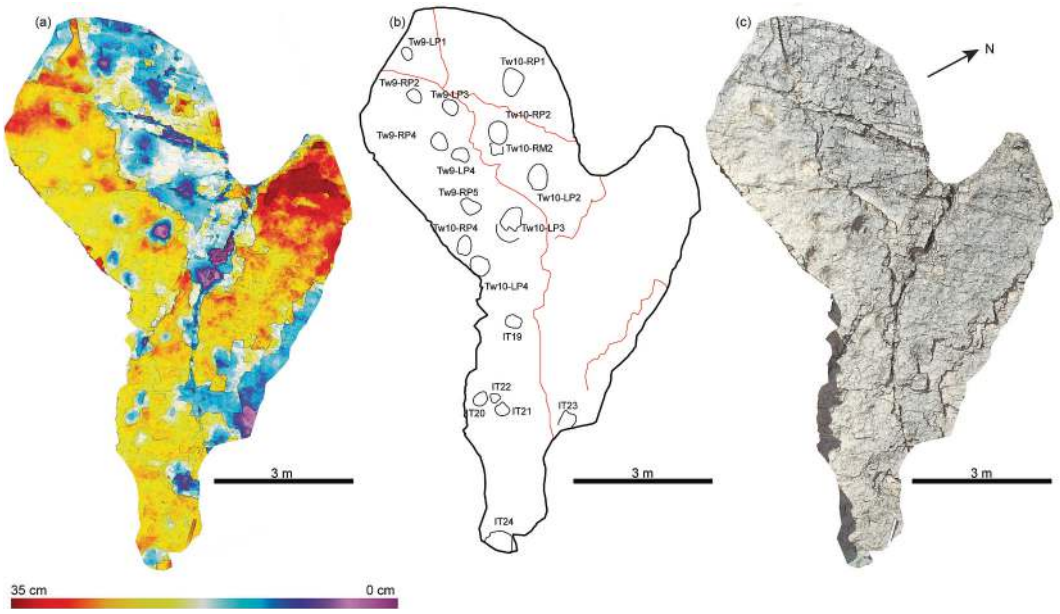


**Fig. 13.** Overview of lower part of QA21. (a) Surface photo; (b) outline drawing; (c) false-colour depth map. Scale bar is 3 m.

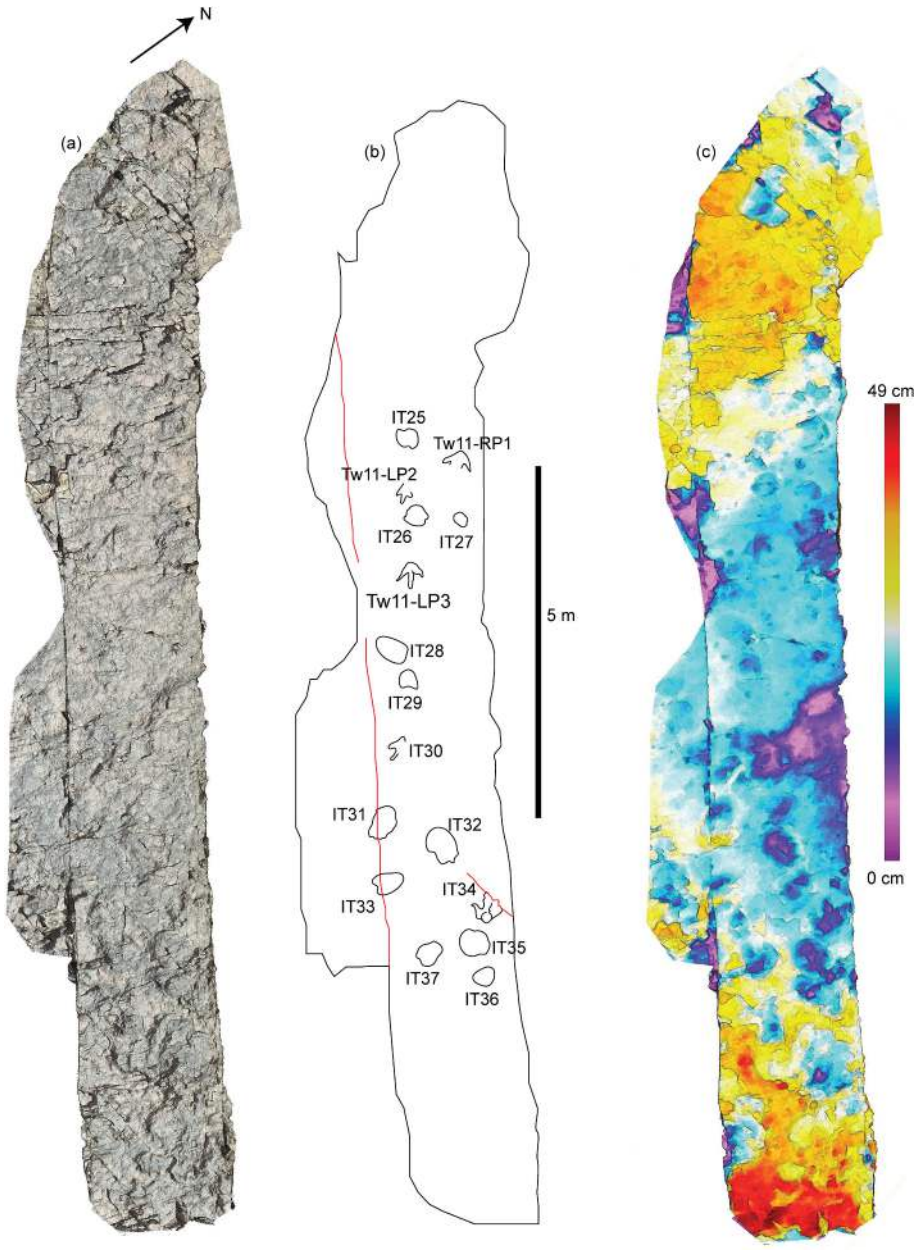


**Fig. 14.** Overview of upper part of QA21. (a) Surface photo; (b) outline drawing; (c) false-colour depth map. Scale bar is 5 m.

footprint length (avg. FL 48.38 cm) suggests this hypothesis. This morphotype has the best preservation of all those described in this study and allows discrimination of the main anatomical features (pad impressions, pad formula and claw marks). The ichnotaxon that resembles Morphotype II the most is *Abelichnus astigerrae* (Calvo, 1991). It has been described as a large-sized tridactyl footprint. Digits are longer than wide, with pad and claw impressions. Digit III is the longest, followed in dimension by digits IV and II. The digits point outwards, except for digit III. Trackways display a pace angulation of about 150°. A significant difference between *Abelichnus astigerrae* and Morphotype II is the length of the digits. Both show digit III as being the longest, but Morphotype II has a longer digit II than digit IV while *Abelichnus astigerrae* seems to show the opposite pattern (Fig. 19). Despite these differences, a new ichnotaxon cannot be defined because of the low number of tracks and the short segments of the trackways. As such, these tracks are assigned to cf. *Abelichnus*.

Evidence of theropod gregarious behaviour in South America are reported from different localities (Calvo and Mazzetta, 2004; Moreno et al., 2012; Pazos et al., 2012; Calvo and Rivera, 2018; Heredia et al., 2020). Based on the similar trackway and track parameters, Tw6 and Tw7 (Fig. 11) could be the second example of synchronized walking in large-sized theropods from the Chacarilla Fm., the first having been reported by Rubilar-Rogers (2008). The two parallel trackways and their identical preservation may suggest the gregarious behaviour of the theropod trackmaker. However, it is also possible that the two different individuals walked in the same direction (Tw7 oversteps Tw6) at different moments, separated only by a short time interval, as the preservation and fidelity are identical. Given the data observed, it is not possible to discern between these two hypotheses. A gregarious behaviour is favoured by the identical orientation of Tw6 and Tw7.

### 5.1.3. Morphotype III

Comparisons for the elongated Morphotype III were restricted to ichnotaxa that show metatarsal impressions, since it is a distinctive feature (Fig. 20). The considered ichnotaxa therefore were: *Picunichnus benedettoi* (Calvo, 1991), *Picunihcnus quijadaensi* (Melchor et al., 2019),

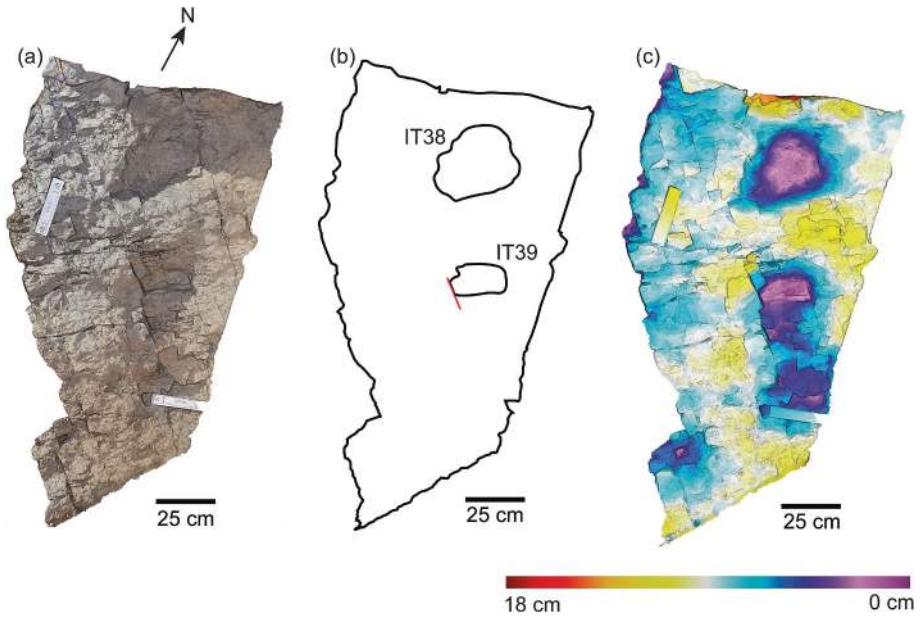


**Fig. 15.** Overview of QA22. (a) Surface photo; (b) outline drawing; (c) false-colour depth map. Scale bar is 25 cm.

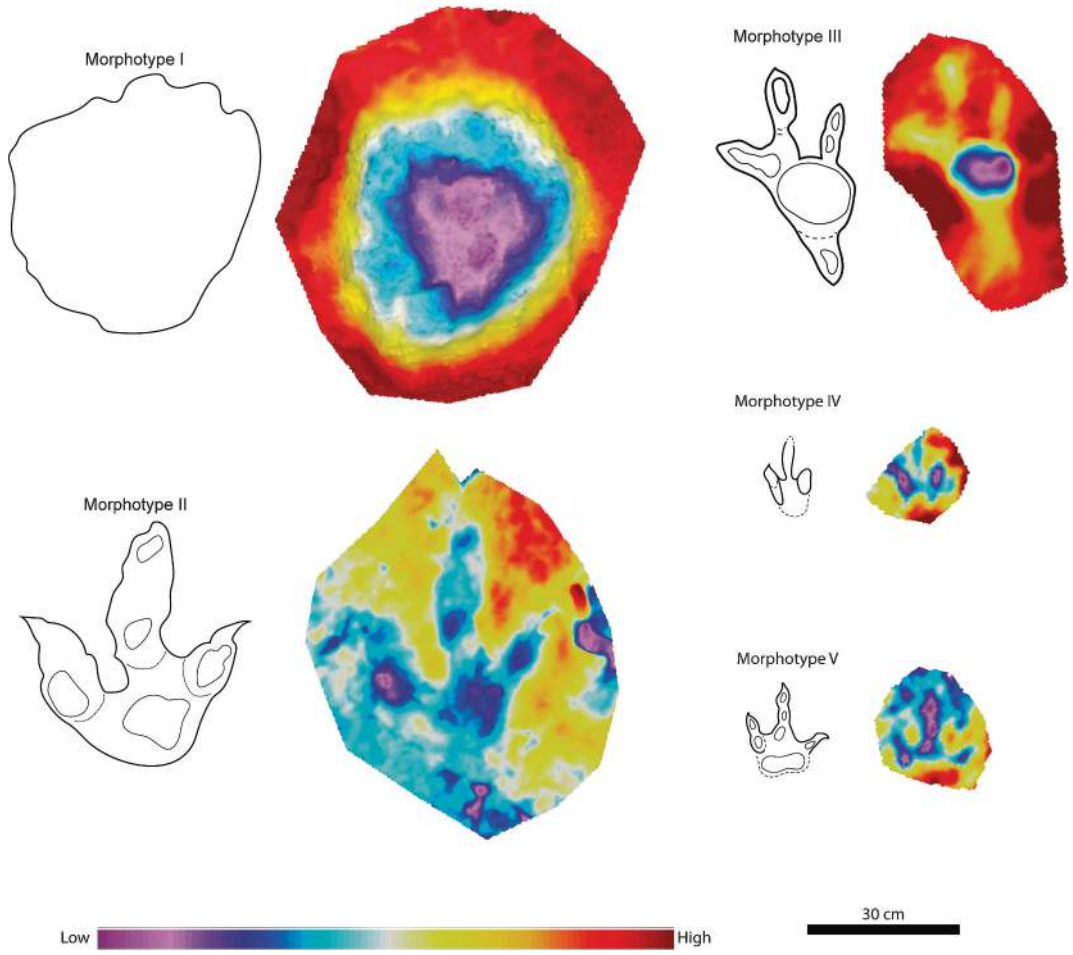


**Fig. 16.** Drawings and false-colour depth maps of all the morphotypes described in this paper. All tracks drawn at the same scale.

*Jialingpus yuechiensis* (Zhen et al., 1983), *Changpeipus carbonicus* (Young, 1960), *Eutynichnium lusitanicum* (Nopcsa, 1923), *Irenesauripus mclearni* (Sternberg, 1932) and *Bueckeburgichnus maximus* (Kuhn, 1958).

The morphological comparison between Morphotype III, *Picunichnus quijadaensi* and *Picunichnus benedettoi* shows similarities, even if they plot separately (Fig. 21). The two tracks have disparate track

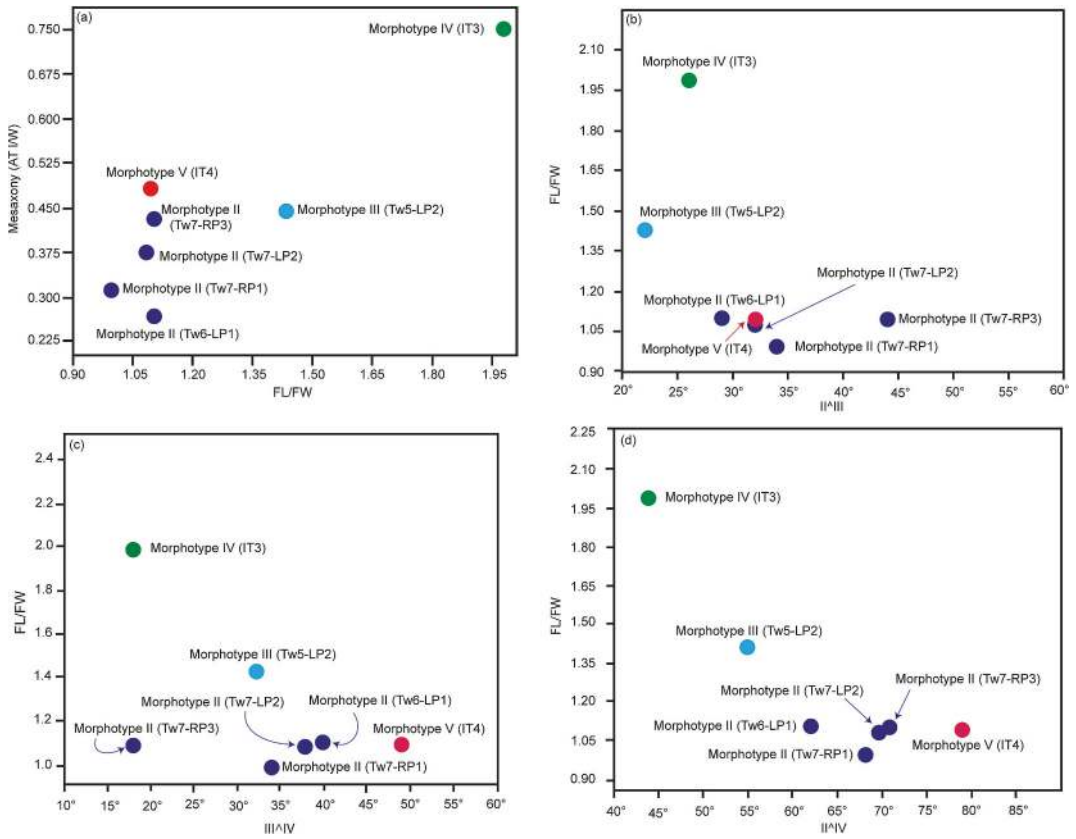


**Fig. 17.** Bivariate graph plotting the footprint length/footprint width ratio of the tridactyl morphotypes against: (a) AT l/w ratio, for the tridactyl morphotypes; (b) interdigital angle IIˆIII; (c) interdigital angle IIIˆIV; (b) total divarication angle IIˆIV.

parameters. The main difference is their digit divergence, where in *Picunichnus benedettoi* it is low while in Morphotype III it is higher (IIˆIII of 22° and IIIˆIV of 23° and 32°). Morphotype III is about twice the size of *Picunichnus benedettoi*. Digit dimensions are quite different since *Picunichnus benedettoi* has a larger digit II than IV while Morphotype III has digits of similar dimensions. However, this comparison is based on just one track (Tw5-LP2) that has both digits preserved. Considering the ichnotaxon *Picunichnus quijadaensi* instead, differences are present in the divarication angle IIˆIV (avg. is 55° for Morphotype III and 32° for per *Picunichnus quijadaensi*) and the hallux impression of Morphotype III lacks a claw mark, which is a distinctive feature for *Picunichnus quijadaensi* (Melchor et al., 2019).

The morphometrical comparisons shows a close relationship with *Changpeipus carbonicus* (Fig. 21). Morphotype III and *Changpeipus carbonicus* are similar in FL and FW (data from Xing et al., 2014 for *Changpeipus carbonicus*) and of course show a similar AT l/w ratio. Otherwise, morphological comparisons between those two tracks (Fig. 20) show significant differences. Morphotype III has a more impressed metatarsal impression and more pronounced digit divergence.

The presence of a penetrating metatarsal impression can be linked to various mechanisms (e.g. dragging of digits, retroverted halluces, forward sliding of the foot on a slippery substrate Lallensack et al., 2021), or due to the same depth of the metatarsal impression and track, visible from false-colour depth maps (Fig. 7). The hypothesis of a greater penetration/sinking of the track on the substrate (Belvedere and Mallison, 2014; Kuban, 1989) is supported. A walking behaviour with greater sinking of the pes in a saturated sediment also seems to be confirmed. This is because the pes and the metatarsal impression are at the same depth in all tracks. The arrangement on the surface tracks, equally spaced and aligned with the midline of the track (e.g. Citton et al., 2015), points to this impression mode. In cases where the metatarsal impressions are associated with a crouching/resting behaviour (Lockley et al., 2003; Milàn et al., 2008; Milner et al., 2009; Nicosia et al., 2007), details like tail impressions, digit I or left and right track side-by-side are usually present but are missing from Morphotype III. This is why those elongated tracks were excluded from the morphological and morphometrical comparison with Morphotype III. Despite behavioural and locomotory considerations, the lack of consistent fits with any other ichnotaxa, both morphologically and morphometrically, make the tracks from Morphotype III unassignable.

### 5.1.4. *Morphotypes IV and V*

The ichnotaxonomic classification of the isolated track composing Morphotype IV and Morphotype V was undertaken by comparing them with the ichnogenera of comparable size studied by Melchor et al. (2019). The integration of our values with those in the supplementary material of Melchor et al. (2019) is plotted in Fig. 22. The morphotypes fall into two distinct ichnofamilies: Grallatoridae (Morphotype IV) and the *Kayentapus*-like group (Morphotype V). For those two morphotypes, a more accurate ichnotaxonomic classification was constrained by the lack of a consistent number of tracks (only one for each morphotype), rather than a deficiency in track preservation.

## 5.2. *Trackmaker identification*

To identify trackmakers (Fig. 23), all different morphotypes were compared with the Late Jurassic-Early Cretaceous skeletal record of South America, accessible via PaleoDB (https://paleobiodb.org). The sauropod record was compared to the occurrences of the superfamily Diplodocoidea and the family Titanosauroidea. For theropods, the record consists of the families Abelisauridae, Spinosauridae and Carcharodontosauridae. The Spinosauridae were excluded (de França et al., 2022; Martill et al., 1996; Sales et al., 2017). Although we still do not

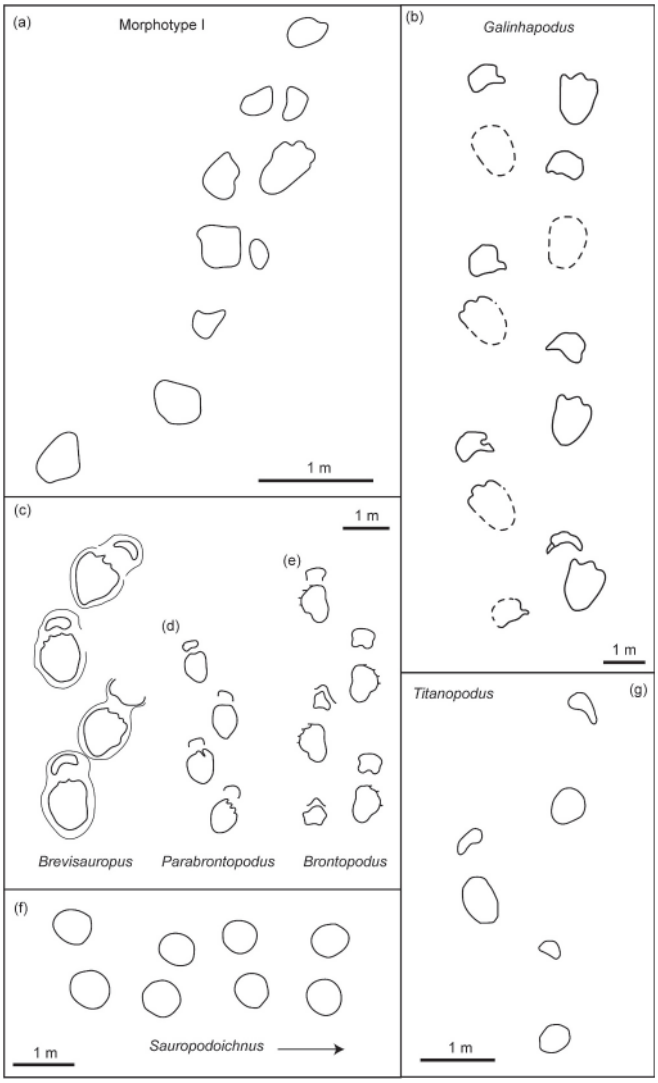


**Fig. 18.** Morphological comparison between Morphotype I (a) and the other ichnogenera. *Galinhapodus* (b) redrawn from Santos et al. (2009). *Brevipodus* (c), *Parabrontopodus* (d) and *Brontopodus* (e) redrawn from Marty et al. (2010). *Sauropodichnus* (f) redrawn from Calvo (1991). *Titanopodus* (g) redrawn from González-Riga and Calvo (2009).

know whether spinosaurids were fully aquatic (Ibrahim et al., 2020) or partially adapted to life in water (Sereno et al., 2022), they in either case do not fit the distal alluvial plain setting of the Chacarilla Fm.

### 5.2.1. *Morphotype I*

The Late Jurassic to Early Cretaceous sauropod record is represented in South America by the superfamily Diplodocoidea and the family Titanosauridae (e.g. Gallina et al., 2014; Pol et al., 2022; Salgado et al., 2015). As the gauge parameter is the only parameter available, the identification of a possible trackmaker stands on shaky ground. It has been shown that trackway gauge is not a valid parameter to differentiate between those groups (Meyer et al., 2018). The trackmaker of this morphotype can be either a diplodocid or a titanosaurid.

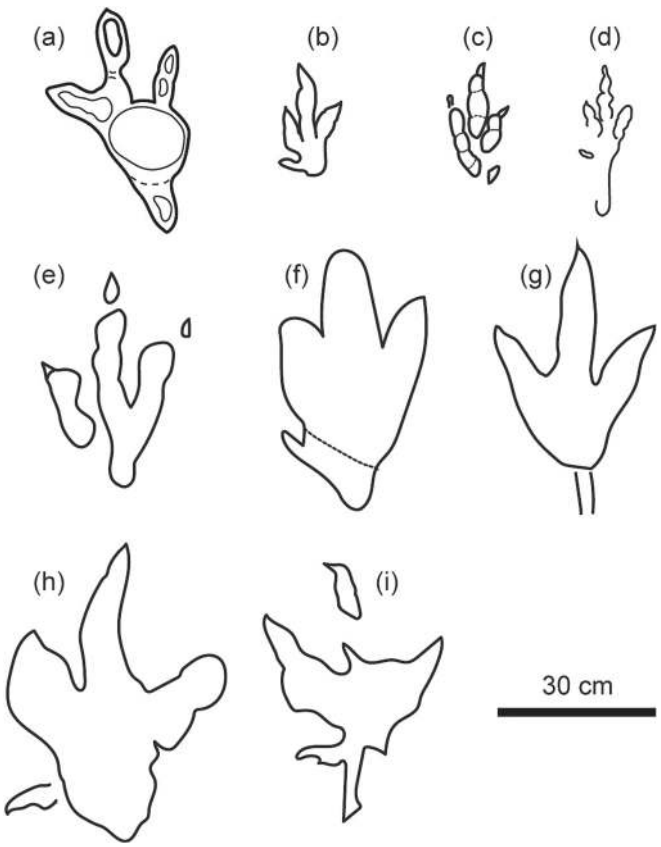


**Fig. 20.** Comparison among outline drawings of Morphotype III (a) and the other ichnotaxa. *Picunichnus quijadaensi* (b) redrawn from Melchor et al. (2019), *Picunichnus benedettoi* (c) redrawn from Calvo (1991), *Jialingpus yuechiensis* (d) redrawn from Xing et al. (2014), *Changpeipus carbonicus* (e) redrawn from Lockley et al. (2013), *Eutynichnium lusitanicum* (f) redrawn from Razzolini et al., 2017, *Irenesauripus mclearni* (g) redrawn from Razzolini et al., 2017, *Bueckeburgichnus maximus* (h) redrawn from Razzolini et al., 2017, and Morphotype 2D (i) redrawn from Belvedere, 2008. All tracks drawn at the same scale. Scale bar is 30 cm.

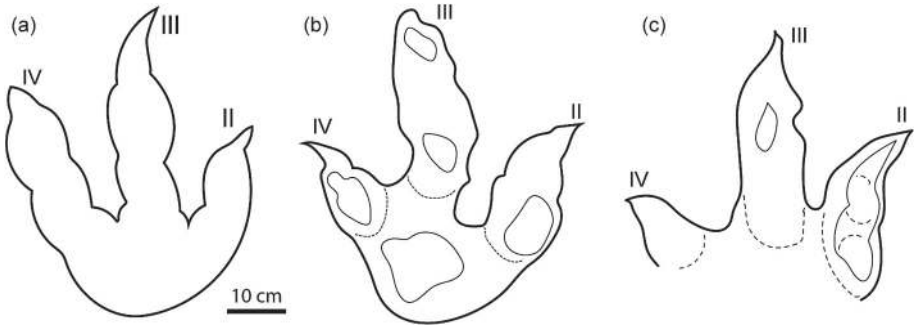


**Fig. 19.** Comparison between: (a) holotype of *Abelichnus astigerrae* redrawn from Calvo (1991), (b) Tw7-RP3 and (c) IT10. Originally right tracks (Tw7-RP3 and IT10) have been mirrored to look left like the holotype. All tracks drawn at the same scale.

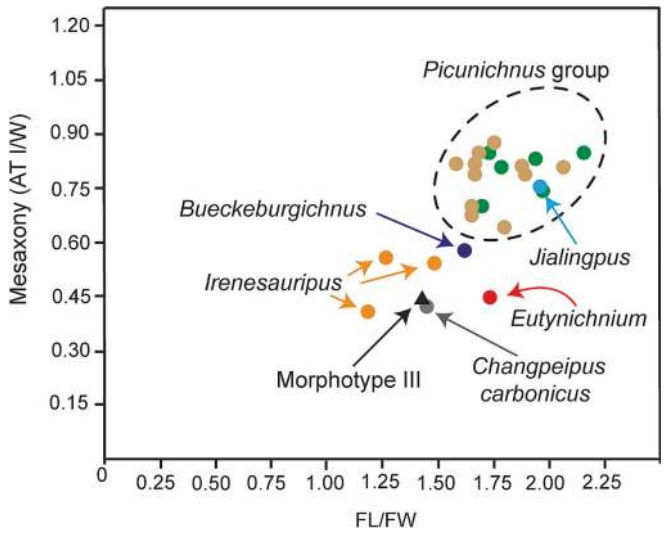


**Fig. 21.** Bivariate graph plotting AT l/W ratio vs. FL/FW ratio for Morphotype III (black triangle), *Eutynichnium lusitanicum* (red dot), *Irenesauripus mcleari* (orange dot) and *Bueckeburgichnus maximus* (blue dot), *Changpeipus carbonicus* (grey dot), *Picunichnus benedettoi* (green dot) *Picunichnus quijadaensi* (light green dot) and *Jialingpus yuechiensis* (light blue dot). (For interpretation of the references to colour in this figure legend, the reader is referred to the web version of this article.)

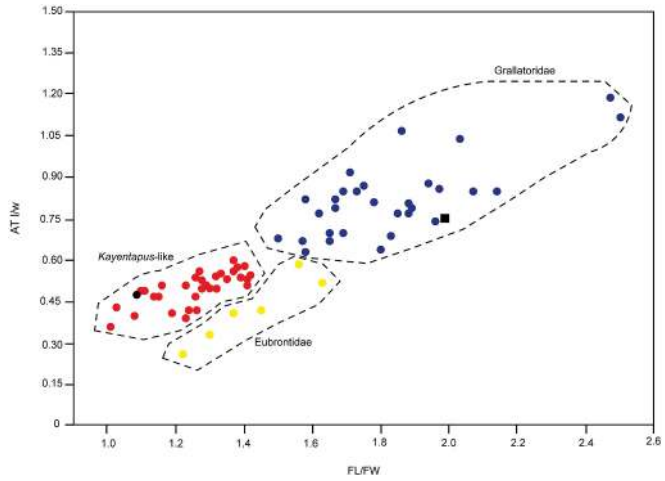


**Fig. 22.** Bivariate graph plotting AT l/W ratio vs. FL/FW ratio of Morphotype IV (black square) and Morphotype V (black dot) with other track groups taken from Melchor et al. (2019).

### 5.2.2. Morphotype II

This morphotype displays a footprint length (avg. FL 36.05 mm) indicative of a large-sized theropod. As stated before (see Section 5.1.2), this morphotype is ichnotaxonomically close to *Abelichnus astigerrae*. The tracks of *Abelichnus astigerrae* were identified by Calvo (1999) as having been left by *Giganotosaurus carolinii*. The attribution was based on the fact that both tracks of *Abelichnus astigerrae* and skeletal remains of *Giganotosaurus carolinii* occur in the same formation (Rio Limay Fm.) in close stratigraphic levels. Other large theropod dinosaurs from the Ceratosauridae (Rauhut and Pol, 2021) and Abelisauridae families also coexisted during this period. Based on the evidence, Morphotype II is best explained by a large Carcharodontosauridae theropod.

### 5.2.3. Morphotype III

This morphotype exhibits a footprint length (avg. FL 36.05 cm) that can be ascribed to a medium-sized theropod trackmaker. In this time interval, medium-sized theropods are known to belong to the abelisaurids and carcharodontosaurids, although further assumptions cannot be made, due to the absence of substantial evidence.

### 5.2.4. Morphotype IV and Morphotype V

These morphotypes exhibit a similar footprint length (FL = 16 cm for Morphotype IV and FL = 18.2 cm for Morphotype V), which can be attributed to the presence of small-sized theropods. The possible trackmakers could be tyrannosauroids (e.g. Kellner, 1999); noasaurids (e.g. Brownstein, 2021; de Souza et al., 2021); Tetanurae (e.g. Rauhut and Pol, 2017) or also the enigmatic *Chilesaurus diegosaurezi* (Baron and Barrett, 2017; Baron, 2024: Novas et al., 2015).

## 6. Conclusions

The Chacarilla Fm. is a well-known dinosaur track-bearing formation from the Late Jurassic to Lower Cretaceous of Chile. The succession studied at the Quebrada de Arcas demonstrates the significance of employing modern ichnological methodologies to previously described tracksites, thereby offering new insights into the ichnodiversity of dinosaurs during the Jurassic-Cretaceous transition.

The studied section consists of about 300 m of fine sandstone and siltstone. The sedimentary structures present, including ripple marks, mud cracks, microbial mats and the tracks of both invertebrates and vertebrates, indicate a distal alluvial plain setting for the Chacarilla Fm. Dinosaur tracks occur on 23 different levels along this section, both as true tracks and in cross-section. The description and measurement of the tracks led to the recognition of 5 morphotypes. Sauropod tracks (Morphotype I) were grouped together; due to their poor preservation and those few better-preserved tracks a formal ichnotaxon cannot be allocated. Morphotype I tracks are interpreted as *Parabrontopodus*-like and the trackmaker is a diplodocid or a titanosaurid. Morphotype II fits with the characteristics of *Abelichnus astigerrae* (Calvo, 1991) and is assigned to cf. *Abelichnus*. This is the second report of large theropod tracks from the Chacarilla Fm. The *Abelichnus* tracks in this study are the largest ever described from South America (max footprint length 51 cm). Due to the age of the Chacarilla Fm. (Late Jurassic to Early Cretaceous) the proposal of a track from there being referred to *Abelichnus* may be interpreted in two ways: either the Chacarilla Fm. age is Late Cretaceous, since this ichnogenus is known from the Cenomanian onwards (Calvo, 1991), or the first occurrence of *Abelichnus* is in the Late Jurassic, if the dating for the formation is correct. New chronological data could help to solve this question. However, the trackmaker of Morphotype II is identified as a generic carcharodontosaurid dinosaur, contrary to *Abelichnus*, which is identified as *Giganotosaurus carolinii.* Trackways of Morphotype II offer a novel perspective on the paleoecology of large theropods, suggesting gregarious behaviour in adult carcharodontosaurids. The interpretation of Morphotype III has been done by comparing known tridactyl theropod ichnogenera with metatarsal impressions. Despite the comparison with numerous ichnotaxa, a reliable classification could not be made. A medium-sized theropod is the potential trackmaker. Morphotype IV falls in the Grallatoridae group and Morphotype V falls in the *Kayentapus*-like group, both tracks having been made by small-sized theropods. Since these are isolated and not completely preserved tracks, a further interpretation would have been too imprecise. Nonetheless, both morphotypes have a significant importance, since small to medium sized tridactyl tracks are not common in the Late Jurassic to Early Cretaceous record (Marty, 2008). Various small-sized dinosaurs at the time are known in South America, but a link between those two morphotypes and their trackmaker cannot be found.

## CRediT authorship contribution statement

**Vincenzo Gesualdi:** Writing – original draft, Visualization, Methodology, Investigation, Formal analysis, Conceptualization. **Matteo Belvedere:** Writing – review & editing, Visualization, Supervision,

**Fig. 23.** Paleoartistic reconstruction of the Quebrada de Arcas. Illustration by Joschua Knüppe.

Methodology, Investigation, Funding acquisition, Data curation, Conceptualization. **Marko Yurac:** Writing – review & editing, Project administration, Investigation, Funding acquisition. **Dorothee Hippler:** Writing – review & editing, Supervision, Funding acquisition. **Nejla Hurem:** Investigation. **Christian Salazar:** Supervision, Project administration, Investigation, Funding acquisition. **Javiera Mendez:** Investigation. **Christian A. Meyer:** Writing – review & editing, Supervision, Investigation, Conceptualization.

## Declaration of competing interest

The authors declare that they have no known competing financial interests or personal relationships that could have appeared to influence the work reported in this paper.

## Acknowledgements

We would sincerely thank: Consejo de Monumentos Nacionales for the research permit (Ord. CMN 1867-2023), SERNAGEOMIN geologist Fernando Sepulveda for bringing to our attention the presence of new tracks in the Quebrada de Arcas and for providing useful information about the geological setting of the area, the Aymara community, Joschua Knüppe for his paleoartistic illustration, palynologists Gabriele Niccolini and Adele Bertini of the University of Florence for analysing the sample for palynomorphs, Dr. E. Mujal and the two other anonymous reviewers for their helpful reviews and suggestions. Jeff Liston for reviewing the English.

VG and MB were funded by the DST “Internationalisation Grants”. MY was funded by the Jurassic Foundation grant. CAM was funded by Professional Paleontological Consulting. DH and NH were funded by the Austrian Academy of Sciences (ÖAW).

## Appendix A. Supplementary data

Supplementary data to this article can be found online at https://doi.org/10.1016/j.palaeo.2025.113088.

## Data availability

Data will be made available on request.

## References

Aguilef, C., Franco, C.M., Tomlison, A., Blanco, N., Alvarez, J.N., Montecino, D.J., Gardeweg, P., Campos, V.P., Rodriguez, C.S., Maksaev, V.J., Bobadilla, H.R., Vasquez, P.I., Grunder, A.L., Dilles, J.H., 2019. Geologia del area Quehuita-Chela. Region de Tarapaca y Antofagasta. Carta Geologica de Chile. Escala 1:100000.

Alexander, R.M., 1976. Estimates of speed of dinosaurs. Nature 261, 129–130.

Apesteguía, S., Gallina, P.A., 2011. Tunasniyoj, a dinosaur tracksite from the Jurassic-Cretaceous boundary of Bolivia. An. Acad. Bras. Cienc. 83, 267–277. https://doi.org/10.1590/S0001-37652011000100015.

Baron, M.G., 2024. The effect of character and outgroup choice on the phylogenetic position of the Jurassic dinosaur *Chilesaurus diegosaurezi*. Palaeoworld 33, 142–151. https://doi.org/10.1016/j.palwor.2022.12.001.

Baron, M.G., Barrett, P.M., 2017. A dinosaur missing-link? *Chilesaurus* and the early evolution of ornithischian dinosaurs. Biol. Lett. 13. https://doi.org/10.1098/rsbl.2017.0220.

Belvedere, M., 2008. Ichnological researches on the Upper Jurassic dinosaur tracks in the Iouaridène area (Demnat, central High-Atlas, Morocco).

Belvedere, M., Farlow, J.O., 2016. A Numerical Scale for Quantifying the Quality of Preservation of Vertebrate Tracks, pp. 93–98.

Belvedere, M., Mallison, H., 2014. Metatarsal impressions in modern ratites: gait, behaviour and posture influences. Geol. Q. 54, 367–380.

Blanco, N., Tomlison, A., 2013. Carta Huatacondo, Región de Tarapacá. Servicio Nacional de Geología y Minería, Carta Geológica de Chile, Serie Geología Básica 156, 1 Mapa Escala 1:100.000.

Blanco, N., Tomlinson, A., Moreno, K., Rubilar, Y., 2000. Importancia estratigrafica de las icnitas de dinosaurios presentes en la Formacion Chacarilla (Jurasico-Cretacico inferior), Region de Tarapaca, Chile. In: IX Congreso Geologico Chileno. Servicio Nacional de Geologia Y Mineria, pp. 1–5.

Brownstein, D.C., 2021. Dinosaurs from the Santonian-Campanian Atlantic coastline substantiate phylogenetic signatures of vicariance in Cretaceous North America. R. Soc. Open Sci. 8. https://doi.org/10.1098/rsos.210127.

Calvo, J.O., 1991. Huellas de dinosaurios en la Formación Río Limay (Albiano-Cenomaniano?), Picún Leufú, Provincia del Neuquén, República Argentina (Ornithischia-Saurischia: Sauropoda-Theropoda). Ameghiniana 28, 241–258.

Calvo, J.O., 1999. Dinosaurs and other vertebrates of the Lake Ezequiel Ramos Mexía Area, Neuquén-Patagonia, Argentina. In: Prooceding of the Second Gondwanan Dinosaur Symposium.

Calvo, J.O., Mazzetta, G., 2004. Nuevos hallazgos de huellas de dinosaurios en la Formación Río Limay (Albiano-Cenomaniano), Picún Leufú, Neuquén, Argentina. Ameghiniana 41, 1–11.

Calvo, J.O., Rivera, C., 2018. Huellas de dinosaurios en la costa oeste del embalse Ezequiel Ramos Mexía y alrededores (Cretácico Superior, Provincia de Neuquén, República Argentina). Bol. Soc. Geol. Mex. 70, 449–497. https://doi.org/10.18268/BSGM2018v70n2a11.

Casamiquela, R.M., Fasola, A., 1968. Sobre pisadas de dinosaurios del Cretacico Inferior de Colchagua (Chile), 30. Universidad de Chile. Facultad de Ciencias y Matematica. Deparamento de Geologia, pp. 1–24.

Charrier, R., Pinto, L., Pía Rodríguez, M., 2007. Tectonostratigraphic evolution of the Andean Orogen in Chile. Geol. Soc. Lond. Spec. Publ. 3, 21–114.

Citton, P., Nicosia, U., Nicolosi, I., Carluccio, R., Romano, M., 2015. Elongated theropod tracks from the Cretaceous apenninic carbonate platform of Southern Latium (Central Italy). Palaeontol. Electron. 18. https://doi.org/10.26879/578.

Cox, R., Lowe, D.R., Cullers, R.L., 1995. The influence of sediment recycling and basement composition on evolution of mudrock chemistry in the southwestern United States. Geochim. Cosmochim. Acta 59, 2919–2940. https://doi.org/10.1016/0016-7037(95)00185-9.

de França, T.C., Santos Brilhante, N., de Oliveira Monteiro Nobre, Y., Alfredo Medeiros, M., Matos Lindoso, R., Rodrigues Costa, F., 2022. The first record of a spinosaurid pedal ungual from Brazil (Boca do Forno Ravine, Itapecuru Formation, Parnaíba Basin). Hist. Biol. 34, 1817–1826. https://doi.org/10.1080/08912963.2021.1981890.

de Souza, G.A., Soares, M.B., Weinschütz, L.C., Wilner, E., Lopes, R.T., de Araújo, O.M. O., Kellner, A.W.A., 2021. The first edentulous ceratosaur from South America. Sci. Rep. 11. https://doi.org/10.1038/s41598-021-01312-4.

de Valais, S., Filippi, V., Molinas, S., Souberlich, R., 2012. Descripción de una huella de terópodo de la Formación Misiones: primer fósil mesozoico fidedigno de Paraguay. Andean Geol. 39, 541–547. https://doi.org/10.5027/andgeoV39n3-a09.

Dutuit, J.M., Ouazzou, A., 1980. Decouverte d'une piste de dinosaure sauropode sur le site d'empreintes de Demnat (Haut-Atlas Marocain). Mem. Soc. Geol. Fr. 139, 95–102.

Falkingham, P.L., Bates, K.T., Avanzini, M., Bennett, M., Bordy, E.M., Breithaupt, B.H., Castanera, D., Citton, P., Díaz-Martínez, I., Farlow, J.O., Fiorillo, A.R., Gatesy, S.M., Getty, P., Hatala, K.G., Hornung, J.J., Hyatt, J.A., Klein, H., Lallensack, J.N., Martin, A.J., Marty, D., Matthews, N.A., Meyer, C.A., Milàn, J., Minter, N.J., Razzolini, N.L., Romilio, A., Salisbury, S.W., Sciscio, L., Tanaka, I., Wiseman, A.L.A., Xing, L.D., Belvedere, M., 2018. A standard protocol for documenting modern and fossil ichnological data. Palaeontology 61, 469–480. https://doi.org/10.1111/pala.12373.

Farlow, J.O., Pittman, J.G., Hawthrone, J.M., 1989. *Brontopodus birdii*, Lower Cretaceous sauropod footprints from the U.S. Golf coastal plain. In: Dinosaur Track and Traces, pp. 374–391.

Galli, C., Dingham, R., 1962. Cuadrángulos Pica, Alca, Matilla y Chacarilla, con un estudio sobre recursos de agua subterránea, provincia de Tarapacá. Escala 1:50.000. Geológica de Chile 123, 7–10.

Gallina, P.A., Apesteguía, S., Haluza, A., Canale, J.I., 2014. A diplodocid sauropod survivor from the early cretaceous of South America. PLoS One 9. https://doi.org/10.1371/journal.pone.0097128.

Garcia, F., 1967. Geología del Norte Grande de Chile. In: Symposium sobre el Geosinclinal Andino. Sociedad Geológica de Chile, p. 168.

Gonzalez-Riga, J.B., 2011. Speeds and stance of titanosaur sauropods: analysis of titanopodus tracks from the late cretaceous of Mendoza, Argentina. An. Acad. Bras. Cienc. 83, 279–290. https://doi.org/10.1590/S0001-37652011005000002.

González-Riga, J.B., Calvo, J.O., 2009. A new wide-gauge sauropod track site from the Late cretaceous of Mendoza, Neuquén Basin, Argentina. Palaeontology 52, 631–640. https://doi.org/10.1111/j.1475-4983.2009.00869.x.

Habel, T., Simoes, M., Lacassin, R., Carrizo, D., Aguilar, G., 2023. A contribution to the quantification of crustal shortening and kinematics of deformation across the Western Andes (g~20-22° S). Solid Earth 14, 17–42. https://doi.org/10.5194/se-14-17-2023.

Heredia, A.M., Díaz-Martínez, I., Pazos, P.J., Comerio, M., Fernández, D.E., 2020. Gregarious behaviour among non-avian theropods inferred from trackways: a case study from the Cretaceous (Cenomanian) Candeleros Formation of Patagonia, Argentina. Palaeogeogr. Palaeoclimatol. Palaeoecol. 538, 1–19. https://doi.org/10.1016/j.palaeo.2019.109480.

Herron, M.M., 1988. Geochemical classification of terrigenous sands and shales from core or log data 1. J. Sediment. Res. 58, 820–829. https://doi.org/10.1306/212F8E77-2B24-11D7-8648000102C1865D.

Hurem, N., Mendez, J., Gesualdi, V., Yurac, M., Belvedere, M., Salazar, C., Meyer, C.A., Hippler, D., 2023. Mineralogy and geochemistry of the Majala and Chacarilla Formations in Northern Chile (Atacama Desert): Implications for provenance, tectonic setting and paleoenvironmental conditions. MinWien 2023.

Ibrahim, N., Maganuco, S., Dal Sasso, C., Fabbri, M., Auditore, M., Bindellini, G., Martill, D.M., Zouhri, S., Mattarelli, D.A., Unwin, D.M., Wiemann, J., Bonadonna, D., Amane, A., Jakubczak, J., Joger, U., Lauder, G.V., Pierce, S.E., 2020. Tail-propelled aquatic locomotion in a theropod dinosaur. Nature 581, 67–70. https://doi.org/10.1038/s41586-020-2190-3.

Kellner, A., 1999. Short note on a new dinosaur (Theropoda, Coelurosauria) from the Santana Formation (Romualdo Member, Albian). Northeastern Brazil. Boletim do Museu Nacional. Nova serie geologia 49, 1–8.

Kuban, G.J., Gillette, D.D., Lockeley, G.M., 1989. Elongate dinosaur tracks. In: Dinosaur Tracks and Traces. Cambridge University Press, pp. 57–72.

Kuhn, O., 1958. Die fährten der vorzeitlichen Amphibien und Reptilien. Meisenbach, pp. 1–64.

Lallensack, J.N., Farlow, J.O., Falkingham, P.L., 2021. A new solution to an old riddle: elongate dinosaur tracks explained as deep penetration of the foot, not plantigrade locomotion. Palaeontology 65. https://doi.org/10.1111/pala.12584.

Lallensack, J.N., Leonardi, G., Falkingham, P.L., 2025. Glossary of fossil tetrapod tracks. Palaeontol. Electron. https://doi.org/10.26879/1389.

Leonardi, G., 1987. Glossary amd Manual of Tetrapod Footprint Paleoichnology, pp. 1–137.

Leonardi, G., 1994. Annotated Atlas of South America Tetrapod Footprints (Denovian to Holocene).

Leonardi, G., De Souza Carvalho, I., 2021. Dinosaur Tracks from Brazil: A Lost World of Gondwana. Indiana University Press, pp. 1–462.

Lockley, M.G., 1994. Dinosaur ontogeny and population structure: interpretations and speculations based on fossil footprints. In: Carpenter, K., Hirsch, K.F., Horner, J.R. (Eds.), Dinosaur Eggs and Babies. Cambridge University Press, pp. 347–370.

Lockley, M.G., 2009. New perspectives on morphological variation in tridactyl footprints: clues to widespread convergence in developmental dynamics. Geol. Q. 4, 415–432.

Lockley, M., Farlow, J.O., Meyer, C.A., 1994. *Brontopodus* and *Parabrontopodus* ichnogen. nov. and the significance of wide- and narrow-gauge sauropod trackways. GAIA 10, 135–145.

Lockley, M., Matsukawa, M., Jianjun, L., 2003. Crouching theropods in taxonomic jungles: ichnological and ichnotaxonomic investigations of footprints with metatarsal and ischial impressions. Ichnos 10, 169–177. https://doi.org/10.1080/10420940390256249.

Lockley, M.G., Li, J., Li, R., Matsukawa, M., Harris, J.D., Xing, L., 2013. A review of the tetrapod track record in China, with special reference to type ichnospecies: Implications for ichnotaxonomy and paleobiology. Acta Geologica Sinica (English Edition). https://doi.org/10.1111/1755-6724.12026.

Marchetti, L., Belvedere, M., Voigt, S., Klein, H., Castanera, D., Díaz-Martínez, I., Marty, D., Xing, L., Feola, S., Melchor, R.N., Farlow, J.O., 2019. Defining the morphological quality of fossil footprints. Problems and principles of preservation in tetrapod ichnology with examples from the Palaeozoic to the present. Earth Sci. Rev. 193, 109–145. https://doi.org/10.1016/j.earscirev.2019.04.008.

Martill, D.M., Cruickshank, A.R.I., Frey, E., Small, P.G., Clarke, M., 1996. A new crested maniraptoran dinosaur from the Santana Formation (Lower Cretaceous) of Brazil. J. Geol. Soc. Lond. 153, 5–8. https://doi.org/10.1144/gsjgs.153.1.0005.

Marty, D., 2008. Sedimentology, taphonomy, and ichnology of Late Jurassic dinosaur tracks from the Jura carbonate platform (Chevenez-Combe Ronde tracksite. NW Switzerland): insights into the tidal-flat palaeoenvironment and dinosaur diversity, locomotion, and palaeoecology.

Marty, D., Belvedere, M., Meyer, C.A., Mietto, P., Paratte, G., Lovis, C., Thüring, B., 2010. Comparative analysis of Late Jurassic sauropod trackways from the Jura Mountains (NW Switzerland) and the central High Atlas Mountains (Morocco): Implications for sauropod ichnotaxonomy. Hist Biol 22, 109–133. https://doi.org/10.1080/08912960903503345.

Melchor, R.N., Rivarola, D.L., Umazano, A.M., Nalín Moyano, M., Mendoza Belmontes, F. R., 2019. Elusive Cretaceous Gondwanan theropods: the footprint evidence from Central Argentina. Cretac. Res. 97, 125–142. https://doi.org/10.1016/j.cretres.2019.01.004.

Mendez, J., 2024. Estratigrafía y sedimentología del miembro continental de la Formación Majala (Jurásico Superior) en la Quebrada Huatacondo, Tarapacá, Chile. PhD Thesis. Universidad Mayor.

Mesa, V., Perea, D., 2015. First record of theropod and ornithopod tracks and detailed description of sauropod trackways from the Tacuarembó Formation (Late Jurassic-? Early Cretaceous) of Uruguay. Ichnos: Int. J. Plant Anim. 22, 109–121. https://doi.org/10.1080/10420940.2015.1030075.

Meyer, C.A., Marty, D., Belvedere, M., 2018. Titanosaur trackways from the late cretaceous el Molino formation of Bolivia (Cal orck'o, Sucre). Ann. Soc. Geol. Pol. 88, 223–241. https://doi.org/10.14241/asgp.2018.014.

Milàn, J., Loope, D.B., Bromley, R.G., 2008. Crouching theropod and *Navahopus* sauropodomorph tracks from the Early Jurassic Navajo Sandstone of USA. Acta Palaeontol. Pol. 53, 197–205. https://doi.org/10.4202/app.2008.0203.

Milner, A.R.C., Harris, J.D., Lockley, M.G., Kirkland, J.I., Matthews, N.A., 2009. Bird-like anatomy, posture, and behavior revealed by an Early Jurassic theropod dinosaur resting trace. PLoS One 4. https://doi.org/10.1371/journal.pone.0004591.

Moreno, K., Pino, M., 2002. Dinosaur footprints in the Banos de Flaco Formation (Tithonian-Upper Jurassic), VI Region, Chile: paleoethology and paleoenviroment. Rev. Geol. Chile 29, 191–206.

Moreno, K., Blanco, N., Tomlison, A., 2004. Nuevas huellas de dinosaurios del Jurásico Superior en el norte de Chile. Ameghiniana 41, 535–544.

Moreno, K., De Valais, S., Blanco, N., Tomlinson, A.J., Jacay, J., Calvo, J.O., 2012. Large theropod dinosaur footprint associations in western Gondwana: behavioural and palaeogeographic implications. Acta Palaeontol. Pol. 57, 73–83. https://doi.org/10.4202/app.2010.0119.

Moreno, K., Silva-Salinas, K., Finsterbusch, O., Vidal-Murillo, L., Iglesias, A., Astorga, G. A., Arriagada, J.I., 2024. Tetradactyl footprints and plant material from the Jurassic-Cretaceous boundary, Tarapaca Region, Northern Chile. J. S. Am. Earth Sci. 142. https://doi.org/10.1016/j.jsames.2024.104962.

Moreno-Sánchez, M., Gómez Cruz, A., Gómez Tapias, J., 2011. Report of dinosaur tracks in the Iguaque Fauna and Flora Sanctuary, near to Chiquiza (Boyacá, Colombia). Bol. Geol. 33, 107–118.

Nicosia, U., Petti, F.M., Perugini, G., D'Orazi Porchetti, S., Sacchi, E., Conti, M.A., Mariotti, N., Zarattini, A., 2007. Dinosaur tracks as paleogeographic constraints: new scenarios for the cretaceous geography of the periadriatic region. Ichnos: Int. J. Plant Anim. 69–90. https://doi.org/10.1080/10420940601006859.

Nopcsa, F., 1923. Die Familien der Reptilien. Gebrüder Borntraeger, pp. 1–210.

Novas, F.E., Salgado, L., Suárez, M., Agnolín, F.L., Ezcurra, M.D., Chimento, N.R., De La Cruz, R., Isasi, M.P., Vargas, A.O., Rubilar-Rogers, D., 2015. An enigmatic plant-eating theropod from the Late Jurassic period of Chile. Nature 522, 331–334. https://doi.org/10.1038/nature14307.

Orrego, M., 1992. Estratigrafía y sedimentación de una secuencia Triásico Jurásica expuesta en el cuadrángulo Cerro Yocas, Sierra de Moreno, región de Antofagasta, Chile. Memoria de Título, Universidad Católica del Norte, Departamento de Ciencias Geológicas.

Pazos, P.J., Lazo, D.G., Tunik, M.A., Marsicano, C.A., Fernández, D.E., Aguirre-Urreta, M. B., 2012. Paleoenvironmental framework of dinosaur tracksites and other ichnofossils in Early Cretaceous mixed siliciclastic-carbonate deposits in the Neuquén Basin, northern Patagonia (Argentina). Gondwana Res. 22, 1125–1140. https://doi.org/10.1016/j.gr.2012.02.003.

Pettijohn, F.J., Potter, P.E., Siever, R., 1972. Sand and Sandstone. Springer US. https://doi.org/10.1007/978-1-4615-9974-6.

Pol, D., Gomez, K., Holwerda, F.M., Rauhut, O.W.M., Carballido, J.L., 2022. Sauropods from the Early Jurassic of South America and the Radiation of Eusauropoda, pp. 131–163. https://doi.org/10.1007/978-3-030-95959-3_4.

Rauhut, O.W.M., Pol, D., 2017. A theropod dinosaur from the late jurassic Canadon Formation of Central Patagonia, and the evolution of the theropod tarsus. Ameghiniana. https://doi.org/10.5710/AMGH.12.10.2017.3105.

Rauhut, O.W.M., Pol, D., 2021. New theropod remains from the Late Jurassic Cañadón Calcáreo formation of Chubut, Argentina. J. S. Am. Earth Sci. 111. https://doi.org/10.1016/j.jsames.2021.103434.

Razzolini, N.L., Belvedere, M., Marty, D., Paratte, G., Lovis, C., Cattin, M., Meyer, C.A., 2017. Megalosauripus transjuranicus ichnosp. nov. A new Late Jurassic theropod ichnotaxon from NW Switzerland and implications for tridactyl dinosaur ichnology and ichnotaxomy. PLoS One 12. https://doi.org/10.1371/journal.pone.0180289.

Riding, J.B., 2021. A guide to preparation protocols in palynology. Palynology 45, 1–110. https://doi.org/10.1080/01916122.2021.1878305.

Romano, M., Whyte, M.A., Jackson, S.J., 2007. Trackway ratio: a new look at trackway gauge in the analysis of quadrupedal dinosaur trackways and its implications for ichnotaxonomy. Ichnos: Int. J. Plant Anim. 14, 257–270. https://doi.org/10.1080/10420940601050014.

Romano, M., Citton, P., Avanzini, M., 2018. A review of the concepts of 'axony' and their bearing on tetrapod ichnology. Hist. Biol. 32, 611–619. https://doi.org/10.1080/08912963.2018.1516766.

Rubilar-Rogers, D., 2008. Theropod Dinosaur Trackways from the Lower Cretaceous of the Chacarilla Formation, Chile.

Rubilar-Rogers, D., Otero, R.A., Yury-Yáñez, R.E., Vargas, A.O., Gutstein, C.S., 2012. An overview of the dinosaur fossil record from Chile. J. S. Am. Earth Sci. https://doi.org/10.1016/j.jsames.2012.03.003.

Sales, M.A.F., Liparini, A., de Andrade, M.B., Aragão, P.R.L., Schultz, C.L., 2017. The oldest South American occurrence of Spinosauridae (Dinosauria, Theropoda). J. S. Am. Earth Sci. 74, 83–88. https://doi.org/10.1016/j.jsames.2016.10.005.

Salgado, L., Novas, F.E., Suarez, M., De La Cruz, R., Isasi, M., Rubilar-Rogers, D., Vargas, A., 2015. Late Jurassic sauropods in Chilean Patagonia. Ameghiniana 52, 418–429. https://doi.org/10.5710/AMGH.07.05.2015.2883.

Santos, V.F., Moratalla, J.J., Royo-Torres, R., 2009. New sauropod trackways from the Middle Jurassic of Portugal. Acta Palaeontol Pol 54, 409–422. https://doi.org/10.4202/app.2008.0049.

Santos, V., Moratalla, J., Royo-Torres, R., Belvedere, M., Castanera, D., Ceríaco, L., Mocho, P., Merino, M., Meyer, C., Sciscio, L., 2024. A revised name and new insights into the Middle Jurassic sauropod trackways from Portugal. A correction of Santos et al. 2009. Acta Palaeontol. Pol. 69, 587–590. https://doi.org/10.4202/app.01167.2024.

Sepulveda, F.A., Gonzalez, E., Tomlison, A., 2023. Geología y estructura del cuadrángulo Quebrada Arcas (1:50.000), región de Antofagasta. Chile.

Sereno, P.C., Myhrvold, N., Henderson, D.M., Fish, F.E., Vidal, D., Baumgart, S.L., Keillor, T.M., Formoso, K.K., Conroy, L.L., 2022. Spinosaurus is not an aquatic dinosaur. Elife 11. https://doi.org/10.7554/eLife.80092.

Sternberg, C.M., 1932. Dinosaur tracks from the Peace River, British Columbia. In: Annual Report of the National Museum of Canada for 1930, pp. 59–85.

Thulborn, R.A., 1990. Dinosaur Track. Chapman and Hall, London, pp. 1–410.

Tomaselli, M.B., Ortiz David, L.D., González Riga, B.J., 2021. Paleoenvironmental contexts of South American Cretaceous sauropod tracks. J. S. Am. Earth Sci. 110. https://doi.org/10.1016/j.jsames.2021.103393.

Tomlinson, A., Blanco, N., Maksaev, V., Dilles, J.H., Grunder, A., Ladino, M., 2001. Geología de la Precordillera andina de Quebrada Blanca-Chuquicamata, Regiones I y II ($20^{0}30'$-$22^{o}30'$ S). In: Servicio Nacional de Geología y Minería. Informe Registrado IR-01-20, 2, 20 Mapas Escala 1: 50.000. Santiago, p. 444.

Xing, L., Klein, H., Lockley, M., Wetzel, A., Li, Z.-D., Li, J.-J., Gierlinski, G.D., Zhang, J.-P., Matsukawa, M., Divay, J.D., Zhou, L., 2014. *Changpeipus* (theropod) tracks from the Middle Jurassic of the Turpan Basin, Xinjiang, Northwest China: review, new discoveries, ichnotaxonomy, preservation and paleoecology. Vertebrata Palasiatica 52, 233–259.

Young, C.C., 1960. Fossil footprints in China. Vertebrata Palasiatica 4, 53–67.

Yurac, M., Salazar, C., Meyer, C.A., Belvedere, M., 2022. The Dinosaur Ichnological Record of Northern Chile: A Review and its Potential Development.

Yurac, M., Belvedere, M., Salazar, C., Mendez, J., Meyer, C.A., 2025. A reappraisal of the late Jurassic dinosaur tracks from the Majala Formation in the Huatacondo Area (Tarapacá, Chile). Palaeogeogr. Palaeoclimatol. Palaeoecol.

Zhen, S., Li, Y., Zhen, B., 1983. Dinosaur footprints of Yuechi, Sichuan. Mem. Beijing Nat. Hist. Museum 25, 1–19.